CHEMISTRY
A European Journal

A Journal of
ChemPubSoc Europe

Accepted Article

Title: Asymmetric organocatalyzed aza-Henry reaction of hydrazones: experimental and computational studies

Authors: Raquel Perez Herrera, Isaac G. Sonsona, Juan V. Alegre-Requena, Eugenia Marqués-López, and M. Concepcion Gimeno

To be cited as: *Chem. Eur. J.* 10.1002/chem.202000232

Link to VoR: http://dx.doi.org/10.1002/chem.202000232

Supported by
ACES

WILEY-VCH

10.1002/chem.202000232

WILEY-VCH

Asymmetric organocatalyzed aza-Henry reaction of hydrazones: experimental and computational studies

Isaac G. Sonsona,[a] Juan V. Alegre-Requena,*[a] Eugenia Marqués-López,[a] M. Concepción Gimeno[b] and Raquel P. Herrera*[a]

Dedication ((optional))

Abstract: The first asymmetric catalyzed aza-Henry reaction of hydrazones is presented. In this process, quinine was used as the catalyst to synthesize different alkyl substituted β-nitrohydrazides with ee up to 77%. This ee was improved up to 94% by a further recrystallization and the opposite enantiomer can be obtained using quinidine as catalyst, opening exciting possibilities in fields where the control of chirality is vital, such as the pharmaceutical industry. Additionally, experimental and *ab initio* studies were performed to understand the reaction mechanism. The experimental results revealed an unexpected secondary kinetic isotope effect (KIE) that is explained by the calculated reaction pathway, which shows that the protonation of the initial hydrazone and the C-C bond forming reaction occur during a concerted process. This concerted mechanism makes the catalysis conceptually different to traditional base-promoted Henry and aza-Henry reactions.

Introduction

The nucleophilic enantioselective addition of nitroalkanes to imines (asymmetric aza-Henry or nitro-Mannich reaction) is an efficient C-C bond forming transformation, useful to create chiral synthetic building blocks containing two versatile functional groups: a nitro and an amino groups.[1] To carry out this synthetic strategy, several *N*-protected imines have been prepared and incorporated in a great number of methodologies, including both metal-based and metal-free (organocatalysis) catalytic approaches.[1]

N-Acylhydrazones are considered stable and storable synthetic imine surrogates, which can be easily prepared by condensation of *N*-acylhydrazines with a broad spectrum of aldehydes and ketones.[2] In addition, the resulting products using *N*-acylhydrazones in Mannich reactions could be valuable medicinal targets due to the pharmacological activity that compounds bearing a hydrazide core exhibit (Scheme 1C).[3] To the best of our knowledge, the use of *N*-acylhydrazones in an asymmetric nitro-Mannich reaction has been overlooked in the literature so far. Instead, in catalysis, β-nitroalkylhydrazides have been only synthesized as racemic mixtures by addition of hydrazides to nitroalkene derivatives (aza-Michael reaction).[4] Since it is known that different enantiomers could exhibit different biological properties, the design of new efficient synthetic methods for the production of enantiomerically enriched β-nitroalkylhydrazides is highly desirable.[5] We have pioneered the first asymmetric organocatalyzed aza-Michael protocol to synthesize chiral β-nitroalkylhydrazides.[6] In this reaction, a bifunctional thiourea was employed as the catalyst, affording good stereoselectivity when aryl substituted β-nitroalkenes are used as the initial reagents. However, this process is not efficient to generate alkyl substituted β-nitrohydrazides from β-nitroalkenes (Scheme 1A) and, currently, there is not any efficient catalytic methodology to produce this type of compounds asymmetrically.[7] This lack of precedents motivated us to develop, for the first time, an organocatalytic process to generate enantioenriched alkyl-substituted β-nitrohydrazides. Hence, in this work, we did not follow the chiral synthetic strategies based on aza-Michael transformations used previously.[6] Instead, we have designed a conceptually different protocol starting from *N*-acylhydrazones (Scheme 1B).

[a] Dr. I. G. Sonsona, Dr. J. V. Alegre-Requena, Dr. E. Marqués-López, Prof. Dr. R. P. Herrera
Laboratorio de Organocatálisis Asimétrica. Departamento de Química Orgánica
Instituto de Síntesis Química y Catálisis Homogénea (ISQCH)
CSIC-Universidad de Zaragoza
C/ Pedro Cerbuna, No. 12. E-50009 Zaragoza, Spain
E-mail: raquelph@unizar.es
[b] Prof. Dr. M. Concepción Gimeno
Departamento de Química Inorgánica
Instituto de Síntesis Química y Catálisis Homogénea (ISQCH)
CSIC-Universidad de Zaragoza
C/ Pedro Cerbuna, No. 12. E-50009 Zaragoza, Spain

Supporting information for this article is given via a link at the end of the document.((Please delete this text if not appropriate))

10.1002/chem.202000232

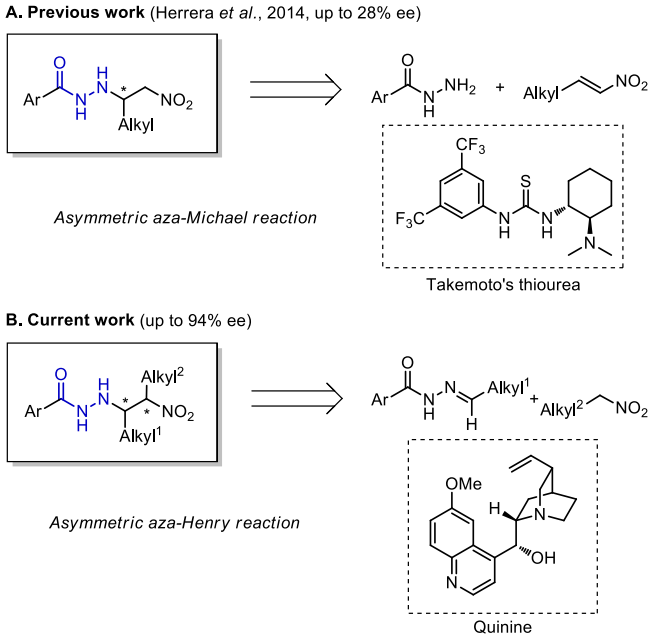

Scheme 1. Asymmetric organocatalyzed approaches for the enantioselective synthesis of *β*-nitroalkylhydrazides.

Results and Discussion

Based on our own experience in the aza-Henry reaction,[8] we envisioned that, in the presence of a chiral basic organocatalyst, nitroalkanes and *N*-acylhydrazones could react to give the desired β-nitroalkylhydrazides. Cinchona alkaloids, which have been extensively employed in organocatalysis,[9] are interesting candidates as catalysts in this process.[10] These chiral natural compounds present some advantages such as low cost and easy functionalization through their hydroxyl substituents.[11] Moreover, we hypothesized that their basic quinuclidine group could contribute to activate the nucleophilic nitroalkane molecule and, at the same time, the chiral structure of this type of catalyst might provide an optimum environment for stereoselective induction. Additionally, the OH group could simultaneously contribute to activate the *N*-acylhydrazone electrophile, since these substrates present different hydrogen bond acceptor sites in their structures that have been previously activated by Lewis acids.[2,12] This plausible bifunctional activation mode could afford good reactivities as well as the adequate transference of chirality from the catalyst to the substrates.

In order to find the best organocatalytic system, the activity of several cinchona-based catalysts (**3a-d**,**g-i**), as well as other bifunctional basic (**3e**,**f**) and acid (**3j**,**k**) organocatalysts, was tested in the model reaction depicted in Scheme 2.

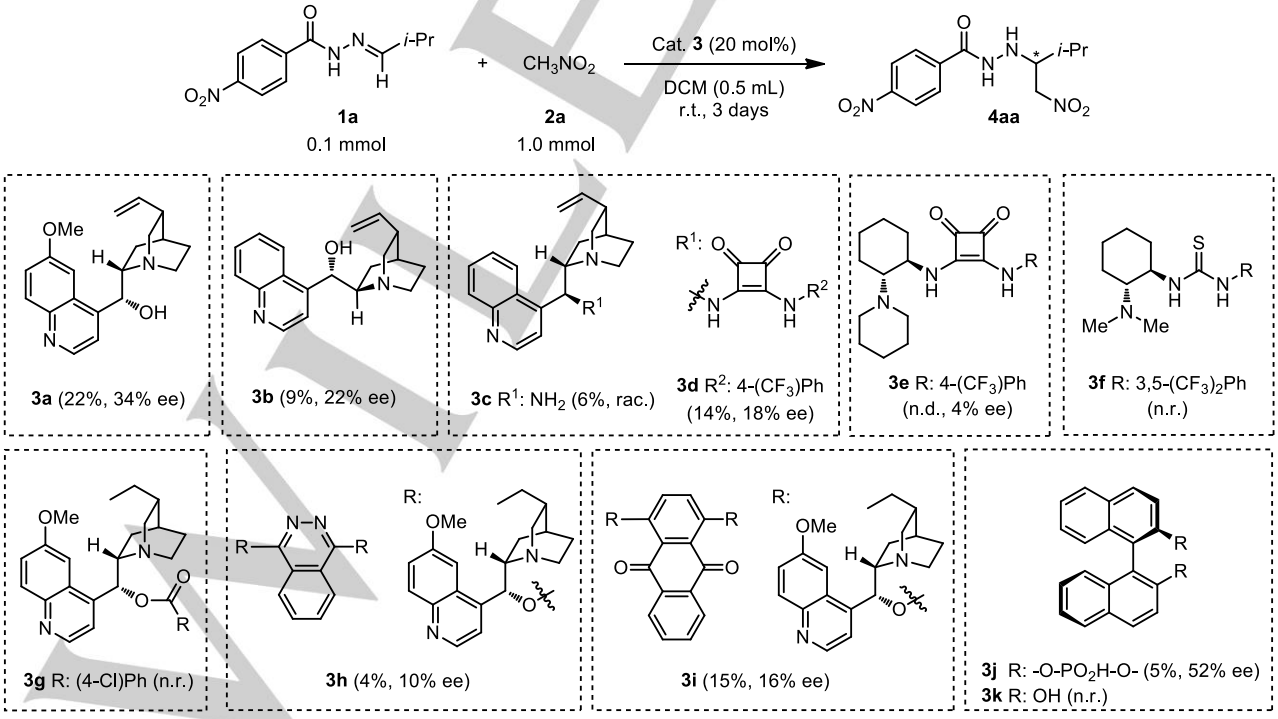

Scheme 2. Catalysts tested in the asymmetric addition of nitromethane (**2a**) to *N*-acylhydrazone **1a**. DCM = dichloromethane; n.r. = no reaction; n.d. = not determined; rac. = racemic mixture; r.t. = room temperature.

Based on the results shown in Scheme 2, the best enantioselectivity (52% ee) was achieved with acid catalyst **3j**. However, this improvement of selectivity was accompanied by a very low yield (5% yield). Additionally, cinchonine (**3b**) and *epi*-cinchonidine derived squaramide **3d** achieved low enantiomeric excesses (22% and 18% ee, respectively). To our delight, cheap quinine alkaloid (**3a**) showed a promising value of enantioselectivity (34% ee) as well as the best reactivity among the catalysts tested (22% yield). Therefore, catalyst **3a** was further explored using different hydrazones **1a-f** under the same reaction conditions (Scheme S1).

The results of this study showed better enantioselectivity and reactivity values for hydrazones bearing electron-withdrawing groups in their phenyl rings (**1a-d**, Scheme S1). With the aim of improving the reactivity and selectivity provided by catalyst **3a**, different parameters of this reaction were studied, such as solvent, catalyst loading and concentration (Table S2). Remarkably, the best reaction conditions were found when using 30 mol% of **3a** and CH_3NO_2 (1 mL) at room temperature (entry 20, Table S2), which led to final product **4aa** with an unprecedented result of selectivity for this compound (40% ee, 57% yield). To study the applicability of this process, the scope using different *N*-acylhydrazones **1a**,**g-n** and nitroalkanes **2a**,**b** was explored (Table 1).

Table 1. Scope of the asymmetric catalyzed aza-Henry reaction of hydrazones **1**.[a]

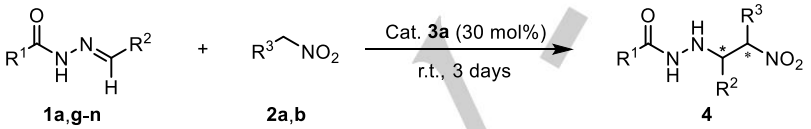

1a,**g-n** **2a**,**b** **4**

Entry	Alkyl *N*-acylhydrazone **1**			Nitroalkane **2**		Product	Yield (%)[b]	d.r.[c]	ee (%)[d]
1	**1a**	R^1: 4-NO_2Ph	R^2: *i*-Pr	**2a**	R^3: H	**4aa**	57	-	40
2	**1g**	R^1: 4-NO_2Ph	R^2: Me	**2a**	R^3: H	**4ga**	91	-	42
3	**1h**	R^1: 4-ClPh	R^2: Me	**2a**	R^3: H	**4ha**	55	-	37
4	**1i**	R^1: 4-BrPh	R^2: Me	**2a**	R^3: H	**4ia**	24	-	39
5	**1j**	R^1: 4-NO_2Ph	R^2: Et	**2a**	R^3: H	**4ja**	79	-	39
6	**1k**	R^1: 4-NO_2Ph	R^2: *n*-Hex	**2a**	R^3: H	**4ka**	79	-	39
7	**1l**	R^1: 4-NO_2Ph	R^2: *i*-Bu	**2a**	R^3: H	**4la**	83	-	40
8	**1m**	R^1: 4-NO_2Ph	R^2: -(CH_2)-Ph	**2a**	R^3: H	**4ma**	74	-	43
9	**1n**	R^1: 4-NO_2Ph	R^2: -$(CH_2)_2$-Ph	**2a**	R^3: H	**4na**	80	-	41
10[e]	**1g**	R^1: 4-NO_2Ph	R^2: Me	**2a**	R^3: H	**4ga**	79	-	45
11[e]	**1n**	R^1: 4-NO_2Ph	R^2: -$(CH_2)_2$-Ph	**2a**	R^3: H	**4na**	32	-	51
12[f]	**1g**	R^1: 4-NO_2Ph	R^2: Me	**2a**	R^3: H	**4ga**	44	-	56 (94)[h]
13[f]	**1n**	R^1: 4-NO_2Ph	R^2: -$(CH_2)_2$-Ph	**2a**	R^3: H	**4na**	18	-	56
14[g]	**1g**	R^1: 4-NO_2Ph	R^2: Me	**2b**	R^3: Me	**4gb**	65	1.4:1	54[i]
15[g]	**1j**	R^1: 4-NO_2Ph	R^2: Et	**2b**	R^3: Me	**4jb**	40	1.7:1	50[i]
16[g]	**1k**	R^1: 4-NO_2Ph	R^2: *n*-Hex	**2b**	R^3: Me	**4kb**	27	2.2:1	72[i]
17[g]	**1l**	R^1: 4-NO_2Ph	R^2: *i*-Bu	**2b**	R^3: Me	**4lb**	25	2.4:1	77[i]
18[g]	**1n**	R^1: 4-NO_2Ph	R^2: -$(CH_2)_2$-Ph	**2b**	R^3: Me	**4nb**	41	1.7:1	73[i]

[a] Nitroalkane **2** (1 mL) is added to a mixture of *N*-acylhydrazone **1** (0.1 mmol) and catalyst **3a** (0.03 mmol). The reaction mixture is stirred at the indicated

temperature during the corresponding reaction time. [b] After isolation of product by column chromatography. [c] Determined by NMR from the reaction mixture. [d] Determined by chiral HPLC analysis (see experimental section). ee after recrystallization is shown between brackets. [e] Reaction carried out at 10 °C for 4 days. [f] Reaction carried out at -20 °C for 5 days, employing a mixture of nitromethane (**2a**):$CHCl_3$ 8:2 as solvent. [g] Reaction carried out at -20 °C during 7 days. [h] The reaction was carried out on higher scale (0.5 mmol of **1g**) and the product isolated by column chromatography was recrystallized in a mixture of ethyl acetate/diethyl ether 1:3, affording **4ga** with 94% ee. [i] Enantiomeric excess provided for the major diastereomer.

In general, the products obtained showed similar enantiomeric excesses for all alkyl substituted hydrazones tested at room temperature (Table 1, entries 1-9). Moreover, we observed that the size of substituent R^2 influences the reactivity of this process in a great extent (entries 1, 2 and 5). Electronic effects of the substituents in the benzoyl group also play an important role in the reaction and affect the reactivity of the process. As envisioned, the presence of electron-withdrawing groups in the aromatic ring of the hydrazone could accelerate the reaction, obtaining the best yield in case of the nitro group (entries 2-4). Carrying out the reaction at lower temperature (–20 °C) affords better results of selectivity but, as expected, lower yields are obtained (entries 2 and 9 *versus* 12 and 13, respectively). Remarkably, when employing a mixture of **2a**:$CHCl_3$ 8:2 as the solvent, **2a** reacts with hydrazone **1g** at –20 °C to produce **4ga** with a moderate yield (44%), showing an appreciable increase of selectivity (entries 2 ,10, and 12). To our delight, we increased the ee of **4ga** to 94% by recrystallization using a mixture of ethyl acetate:diethyl ether 8:2 as solvent (entry 12), which opens new doors to improve the stereocontrol of this reaction in a great extent. Finally, the use of nitroethane (**2b**) afforded moderate to good results of enantioselectivity at –20 °C (entries 14-18, 50-77% ee). Unfortunately, aryl *N*-substituted hydrazones did not react under these reaction conditions, even when very electron withdrawing aryl groups were employed, which is most likely due to the high insolubility of these compounds in $MeNO_2$, CH_2Cl_2 and $CHCl_3$ (Table S3).

In order to know the absolute configuration of our products, single crystals were grown from adduct **4ga** (94% ee) using a mixture of ethyl acetate:toluene 1:1 as solvent. The absolute configuration of this product is *S* when using **3a** as catalyst (Figure 1).[13] We assume the same absolute configuration for all final products. Following an identical procedure, a pure crystal of adduct (*R*)-**4ga** was obtained using quinidine (**3e**) as catalyst, proving that we could easily tune the absolute configuration of the generated chiral center.

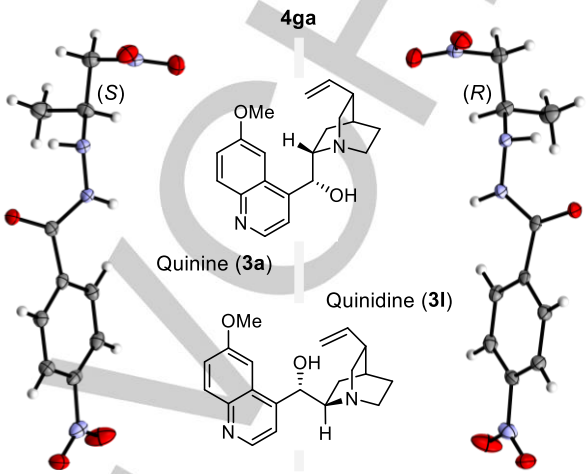

Figure 1. X-ray crystal structure of (*S*)-**4ga** (obtained using **3a** as catalyst) and (*R*)-**4ga** (obtained using **3l** instead of **3a**).

Mechanistic studies

Experimental reaction orders and kinetic isotope effects (KIE) of the reaction

We studied the mechanism of this asymmetric addition of nitroalkanes **2** to hydrazones **1** using kinetic experiments as well as density functional theory (DFT) calculations. Most of the previously reported Henry reactions of aldehydes and aldimines catalyzed by chiral Brønsted bases commonly involve three reactions steps (Scheme 3).[1,14] In the first step, the catalyst deprotonates the nitroalkane substrate, leading to the formation of the corresponding nitronate anion (Scheme 3A). In the second step, the nitronate anion from substrate-catalyst complex **5** attacks to the sp^2 pro-chiral center of the electrophile under stereoselective control (Scheme 3B). This step usually determines the reactivity and selectivity of the process. Finally, the resulting intermediate is protonated in a subsequent step to form the enantioenriched product and the catalyst is regenerated.

10.1002/chem.202000232

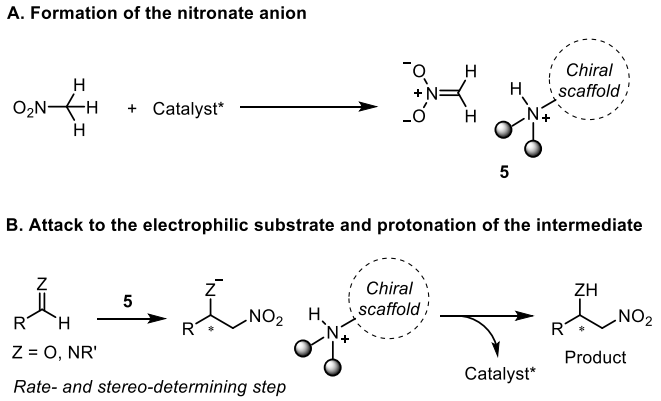

Scheme 3. Previously reported mechanisms of the Henry reaction with aldehydes and imines promoted by chiral basic catalysts. (A) Formation of the nitronate anion. (B) Attack of the nitronate anion to the electrophilic aldehyde or aldimine with the subsequent protonation step.

In a preliminary kinetic study, the concentration of hydrazone **1** over time was monitored by ^{1}H-NMR spectroscopy at 22.5 ºC. We studied the addition of CD_3NO_2 (**2a**) to *N*-acylhydrazone **1h** because this homogeneous reaction presents signals that are easy to track using ^{1}H-NMR techniques (Figure S71).[15] Since the concentration of CD_3NO_2 barely changes during the reaction, this is a pseudo-first order process. The concentration profile of substrate **1h** in the reaction medium (CD_3NO_2/$CDCl_3$ 3:2) (Figure S69), as well as the outcomes of initial rate method experiments (Figure S70, Table 2, entries 1 and 3), suggested that the hydrazone has a reaction order of one. Furthermore, the reaction order of catalyst **3a** was determined to be one by the initial rate method (Table 2, entries 1 and 2).[16] Therefore, these results suggest that there are one molecule of catalyst and one of hydrazone involved in the rate-limiting step/s (RLS) of the reaction.

Table 2. Initial rates study in the asymmetric addition of deuterated nitromethane to hydrazone **1h**.

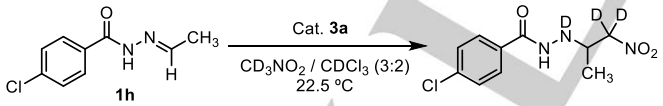

Entry	$[\mathbf{1h}]_o$ (mol·L^{-1})	$[\mathbf{3a}]_o$ (mol·L^{-1})	Initial rate (10^{-7} mol·L^{-1}·s^{-1})	Relative initial rate
1	0.10	0.03	3.80 ± 0.06	1.00
2	0.10	0.06	7.46 ± 0.04	1.96
3	0.05	0.03	1.80 ± 0.07	0.47
4[b]	0.10	0.03	4.97 ± 0.03	1.31

[a] To a solution of hydrazone **1h**, catalyst **3a**, and mesitylene (internal standard, 0.05 mmol) in 200 µL of $CDCl_3$ at 22.5 ºC, 300 µL of deuterated nitromethane was added. The concentration of reagent **1h** *vs* time is monitored by ^{1}H-NMR spectroscopy. [b] The reaction is carried out using nitromethane (**2a**, CH_3NO_2) instead of deuterated nitromethane (CD_3NO_2).

In order to gather more valuable mechanistic information, kinetic isotope effects (KIE) were also measured. For the model reaction previously employed, a ^{2}H KIE (k_H/k_D) of 1.31 (secondary KIE) was observed using CH_3NO_2 and CD_3NO_2 (Table 2, entries 1 and 4). This value is difficult to rationalize based on the previous studies mentioned in Scheme 3, since the RLS of these studies was proposed to be the nitronate attack to the carbonyl or imine group, which would lead to an inverse secondary ^{2}H KIE (k_H/k_D < 1).[17c,d] Also, if the initial deprotonation of **2a** was the RLS, a primary ^{2}H KIE (k_H/k_D > 2) would be expected and, therefore, we can also rule out this possibility.[17a,b]

All the results obtained from these initial kinetic studies suggest that (i) the order of reaction of hydrazones **1** and catalyst **3a** is one and, therefore, one molecule of both species is participating in the RLS, (ii) the reaction follows a different reaction mechanism compared to previous Henry and aza-Henry reactions due to the distinct KIE value observed, and (iii) the RLS does not correspond to the initial step of deprotonation of nitroalkane **2a**. This information is crucial to generate a reliable computational model and will help to evaluate the theoretical outcomes.

Computational study of the mechanism

In order to understand which are the steps and interactions that influence the kinetics and thermodynamic parameters of this process, we carried out a mechanistic computational study using the addition of **2a** to hydrazone **1g** as the model reaction. In the analysis, a significant number of conformations for the catalyst and substrates interacting through different functional groups were considered (42 in total). From all the possible isomers, 13 possible transition states (TSs) were found for the *S* enantiomer (see the ESI for more information). The structures observed in the most favorable **TS-I** systems indicate that electrophile **1g** interacts with the protonated quinuclidine group of the quinine catalyst before the nucleophilic attack of the nitronate takes place (Figure 2A). This model has been suggested previously by Houk and coworkers for other chemical transformations catalyzed by cinchona alkaloids,[18b] and a mechanism with similar interaction mode has been proposed by Paton and coworkers in the Henry reaction of aldehydes catalyzed by chiral phosphazenes.[18a] In contrast, all **TS-I** steps in which the electrophile is interacting with the OH group of the catalyst show considerably higher energies (Figure 2B).[19]

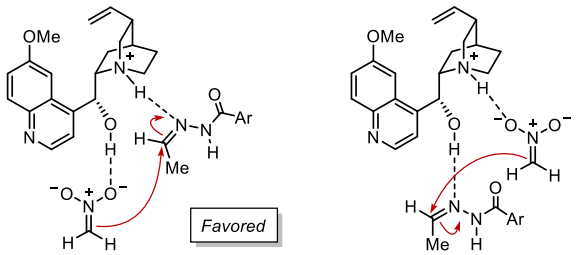

Brønsted acid catalysis (A)
Nine **TS-I** found (G_{rel} from 0.0 to 3.3)

Hydrogen bonding catalysis (B)
Four **TS-I** found (G_{rel} from 4.0 to 9.0)

Figure 2. General different binding modes between quinine and the substrates of the reaction, along with the calculated relative G (G_{rel}, in kcal·mol^{-1}) of individual conformers of **TS-I** for each type of binding mode. Ar = 4-NO_2Ph.

10.1002/chem.202000232

The reaction pathway leading to the enantiomer obtained experimentally (*S*) was studied, including the substrates···catalyst (**Int-I**) and product···catalyst (**Int-II**) complexes formed before and after the C-C bond forming reaction (Figure 3A). Based on the calculated reaction profile, the protonation of the C=N group and the C-C bond forming reaction occur at the same time in a concerted TS (**TS-I**, Figure 3B). Intrinsic reaction coordinate (IRC)[20] calculations and relaxed potential energy surface scans suggest that there might be a stable intermediate between **Int-I** and **TS-I** corresponding to the protonation of hydrazone **1g** before the C-C bond is created (Figure S73). However, this intermediate is found as a stable intermediate only in some conformational pathways while it represents a hidden intermediate[21] in the others. This concerted process is analogous to the basic phosphazene-catalyzed Henry reaction previously reported by Paton and coworkers.[18a] Remarkably, the calculated mechanism might explain the unusual secondary ^{2}H KIE of 1.31 for an aza-Henry reaction observed in the experimental initial rates study (Table 2, entries 1 and 4). Assuming that the initial deprotonation of CH_3NO_2 is a fast process and does not significantly affect the overall ^{2}H KIE, the calculated ^{2}H KIE corresponds to that of **TS-I** and it is 1.65 for the most stable conformer (Figure S75), which is similar to the experimental value. This secondary KIE value suggests that the mechanism is concerted, averaging the mismatching KIE effects of the C-C bond formation (associated with secondary inverse KIEs)[17c] and the protonation of the imine group (causing a primary KIE). It is worth to mention that the catalyst plays an important role in the kinetics of the reaction, since it considerably stabilizes the nitronate nucleophile (**2a**$^-$) compared to the uncatalyzed **2a**:CH_2NO_2H tautomeric equilibrium (Figure 3A, red *versus* black lines).

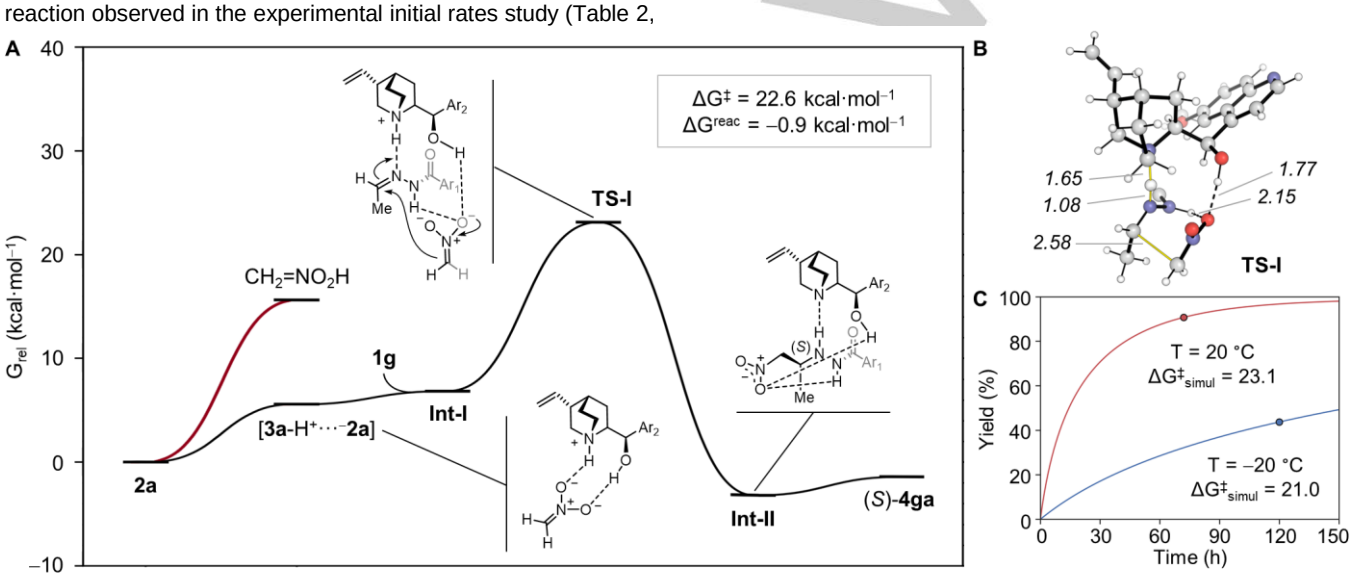

Figure 3. (A) Reaction pathway and energy profile (in kcal·mol^{-1}) of the reaction between nitromethane and hydrazone **1g**. Distances are indicated in Å. Boltzmann weighted Gibbs free energies (G) were calculated using ωB97X-D/Def2-QZVPP//ωB97X-D/6–311G(d) (SMD = CH_3NO_2, T = –20 °C).[22] Quasi-harmonic and concentration corrections were applied to G using *GoodVibes*,[23] assuming concentrations of 1.00 M for **1g**, **3a**, **4ga**, CH_2=NO_2H, intermediates and TSs, and 22.64 M for CH_3NO_2 (solvent). Ar_1 = 4-NO_2Ph, Ar_2 = 6-methoxyquinoline. (B) Representation of the most stable conformer found in **TS-I**. Bonds involved in the transition states are represented with yellow lines. The 4-NO_2PhCO group of **1g** is omitted to allow for a better visualization. (C) Concentration profiles of **1g** and (*S*)-**4ga** obtained with kinetic simulations (using *Berkeley Madonna*, see section *Berkeley Madonna kinetic simulations* in the ESI).[24] $\Delta G^{\ddagger}_{simul}$ = energy of **TS-I** used in the simulation in kcal·mol^{-1}. The two circles represent the experimental yields obtained at 20 and –20 °C.

As expected, the calculated reaction is exergonic by 0.9 kcal·mol^{-1} (Figure 3A). Experimentally, we found that this reaction is kinetically controlled since the retro-Henry reaction was very slow under the conditions employed (Table S4). This is consistent with the calculated profile since the energy barrier of the reverse reaction (from **Int-II** to **TS-I**) is 2.7 kcal·mol^{-1} higher than that of the forward reaction. Therefore, in this Curtin-Hammett scenario,[25] the reaction profile shown in Figure 3A suggests that the rate- and stereo-determining step is **TS-I**, since it is the step that contains the chiral information with highest energy.[26] Further kinetic simulations suggest that the calculated energy profile reproduces significantly well the reactivity observed experimentally at different temperatures (Table 1, entries 2 and 12), since concentration profiles identical to the experimental results (91% yield over three days and 44% yield over five days, at 20 °C and –20 °C, respectively, represented with circles in Figure 3C) are obtained just by slightly adjusting the G of **TS-I** from 22.6 to 23.1 and 21.0 kcal·mol^{-1} (Figure 3C).

Studies regarding the origin of enantioselectivity, based on the differences between the most stable **TS-I** conformers leading to each enantiomer, are very useful in the design of more efficient

catalysts. Unfortunately, in this case, such a comprehensive study does not proceed because the computational study leads to the opposite enantiomer (*R*) compared to experimental findings.

Thus, even though the orders of reaction, KIE, thermodynamic parameters and kinetic profile of the model reaction (using **1g**) match considerably well the experimental data, the absolute configuration observed experimentally (*S*) could not be captured when using different relatively high DFT levels of theory (Table 3, entries 1-7, and Table S6). The calculated $\Delta\Delta G^{\ddagger}$ values differed depending on the level of theory employed ranging from −0.6 to −1.9 kcal·mol^{-1} or 47% to 92% ee. It is worth to mention that (i) we used different solvents to account for potential sources of error from the solvation model based on density (SMD), and (ii) changing the solvent from CH_3NO_2 to CH_2Cl_2 does not practically influence the experimental ee (from 34% to 40% ee when using **1a** and **2a** at r.t., Scheme 2 and Table 1, entry 1). A more extreme example of misleading selectivity predictions is observed when using **1o** (hydrazone with a *t*Bu substituent, which has not been considered experimentally), instead of **1g**.[27] In this case, the uncertainty of DFT methods leads to the prediction of different absolute configurations depending on the method employed (Table 3, entries 8-11, and Table S8). In this example, the $\Delta\Delta G^{\ddagger}$ values also changed depending on the DFT protocol employed (from −0.8 to 1.2 kcal·mol^{-1}). Although the total variation range is only 0.7 kcal·mol^{-1} broader than the previous case (1.3 *versus* 2.0 kcal·mol^{-1} of variation between DFT methods), this time the results lead to predicted ee values that range from 60% of the *R* to 77% of the *S* enantiomer (Table 3, entries 8 and 10, respectively). This study clearly shows that the DFT techniques employed are not suitable to predict enantioselectivity and absolute configuration for this substrate even though the variation range for $\Delta\Delta G^{\ddagger}$ calculations are inside reasonable values for this relatively high-demanding DFT protocols (triple-zeta and quadruple-zeta basis sets with and without diffuse functions, as well as functionals that include dispersion corrections).

Table 3. Enantioselectivity prediction using different DFT methods, solvents and substrates at 20 °C.

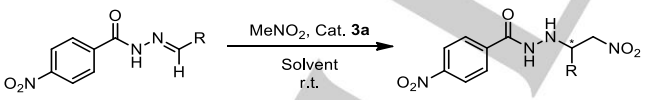

R = Me (**1g**); R = *t*-Bu (**1o**)

Entry	Hydrazone	DFT Method[a]	Solvent[b]	$\Delta\Delta G^{\ddagger}$ (kcal·mol^{-1})[c]	ee (%)[c]
1	**1g**	A	CH_3NO_2	−1.8	−92 (*R*)
2	**1g**	B	CH_3NO_2	−1.2	−77 (*R*)
3	**1g**	C	CH_3NO_2	−1.7	−90 (*R*)
4	**1g**	D	CH_3NO_2	−0.7	−53 (*R*)
5	**1g**	E	CH_3NO_2	−1.9	−92 (*R*)
6	**1g**	F	CH_2Cl_2	−1.3	−80 (*R*)
7	**1g**	G	CH_2Cl_2	−0.6	−47 (*R*)
8	**1o**	A	CH_3NO_2	−0.8	−60 (*R*)
9	**1o**	B	CH_3NO_2	−0.4	−32 (*R*)
10	**1o**	F	CH_2Cl_2	1.2	77 (*S*)
11	**1o**	G	CH_2Cl_2	1.1	73 (*S*)

[a] DFT methods: A = ωB97X-D/6–311G(d); B = ωB97X-D/Def2-QZVPP//ωB97X-D/6–311G(d); C = M06-2X-D3/Def2-QZVPP//ωB97X-D/6–311G(d); D = B3LYP-D3(BJ)/Def2-QZVPP//ωB97X-D/6–311G(d); E = ωB97X-D/6–311++G(d,p); F = B3LYP-D3(BJ)/6–311G(d); G = B3LYP-D3(BJ)/Def2-QZVPP//B3LYP-D3(BJ)/6–311G(d). [b] Solvent used in geometry optimizations and single-point corrections. [c] Calculated using the ee obtained from Boltzmann probabilities of 14 different **TS-I** conformers (seven for each enantiomer), see Tables S6 and S8 for more information.

The prediction of misleading enantioselectivity values and absolute configurations is not surprising since (i) the ee of the model reaction ranges from 42% (at 20 °C, r.t.) to 56% (at −20 °C), which represents $\Delta\Delta G^{\ddagger}$ values of only 0.52 and 0.64 kcal·mol^{-1}, respectively, and (ii) the stereo-controlling step contains a considerable high number of possible conformers, which adds multiple potential error sources to the results (i.e. missing conformers after the conformational search, individual errors of each conformer, etc.). In fact, errors ranging from two to four kcal·mol^{-1} (or even larger) are not uncommon when measuring $\Delta\Delta G^{\ddagger}$ with DFT in other relatively complex systems. A good example to show the limitations of enantioselectivity calculations with DFT is the dioxirane-catalyzed epoxidations studied by Breslow, Friesner and coworkers.[28a] In Table S1 of their ESI, there are many examples in which the error of the calculated $\Delta\Delta G^{\ddagger}$ is larger than two or three kcal·mol^{-1}, which led to the prediction of wrong absolute configurations.[28b] Therefore, the erroneous DFT results observed when predicting absolute configurations in this work could serve as an example that enantioselectivity prediction is not very precise in some complex systems with low or moderate ee. In many cases when studying relatively complex molecular systems, the right absolute configuration might be obtained for the wrong reasons (i.e. since there are only two possible outcomes, *S* and *R*, "randomly predicted" ee values have a 50% probability to lead to the right configuration). The results of this study strongly stress the necessity of comparing computational predictions with experimental data when calculating ee and absolute configurations.

Considering all the kinetic experimental and computational results, a plausible catalytic cycle is proposed for this reaction (Scheme 4). Initially, catalyst **3a** deprotonates the nitromethane (**2a**) through its basic quinuclidine group, leading to the nitronate anion···catalyst complex [**3a**-H$^+$···$^-$**2a**]. Subsequently, hydrazone **1** interacts with [**3a**-H$^+$···$^-$**2a**] to make a new complex including the three reaction components (**Int-I**). Once this ternary complex is formed, the hydrazone molecule is protonated by the N-H$^+$ group of the catalyst at the same time as the C-C bond formation takes place between **1** and the nitronate anion (**TS-I**). As a consequence of the bifunctional activation of both substrates by catalyst **3a**,[29] the nitronate anion attacks hydrazone **1**, leading to a (*S*)-product···catalyst complex (**Int-II**). In the last step, a molecule of nitromethane (**2a**) replaces product **4** in the product···catalyst complex, which regenerates the catalyst and starts a new catalytic cycle.

10.1002/chem.202000232

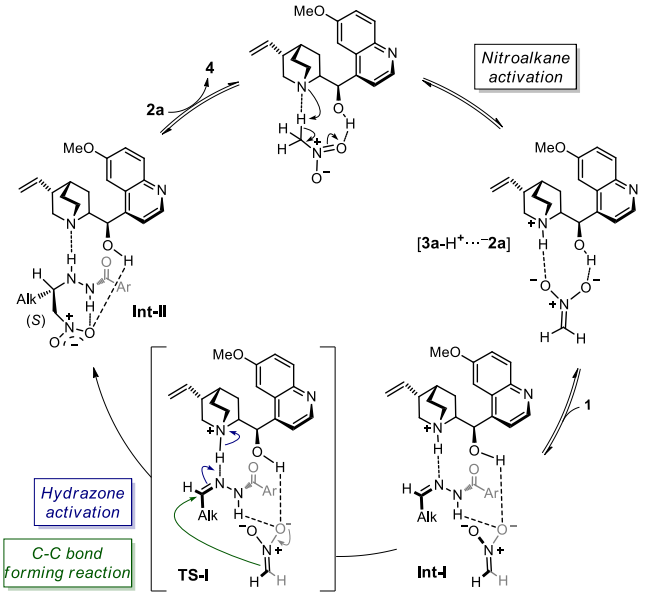

Scheme 4. Proposed catalytic cycle for the asymmetric organocatalyzed addition of nitromethane **2a** to hydrazones **1**.

Conclusions

In this work, the first asymmetric catalytic aza-Henry reaction using hydrazones is reported. This process has proven to be an efficient method to synthesize alkyl substituted β-nitroalkyl hydrazide derivatives with ee up to 77%, which can increase up to 94% after recrystallization. Considering that the maximum value of ee achieved previously was 28%,[6] this new asymmetric protocol might help to generalize the use of these compounds in different fields where using chiral compounds is crucial, such as the pharmaceutical industry. Among the different catalysts tested, the best results were obtained with quinine, which makes this synthetic protocol more appealing since this type of catalyst is relatively cheap and commercially available. Moreover, the use of quinidine let us to obtain the opposite enantiomer, which could be interesting in order to study distinct biological activity of each enantiomer.

Experimental and kinetic studies were carried out in order to gain insight into the reaction mechanism. Interestingly, the results revealed that in the transition state of the enantio-determining and rate-limiting step of the reaction, the hydrazone electrophile is protonated by the catalyst at the same time as the C-C bond forms. This leads to an unexpected experimental and computational secondary KIE. In this step, the catalyst is activating both substrates in a bifunctional fashion, leading to the stereo-controlled attack of nitronate anions to hydrazones **1**.

This work represents an interesting example about the difficulties of computational calculations for estimating small free energy differences.

Experimental Section

General information.

All commercially available solvents and reagents were used as received without further purification. Thin layer chromatography (TLC) analyses were carried out using aluminum sheets recoated with silica gel (60 F_{254}, Merk) and fluorescent-indicator. The spots of compounds were visualized by UV light at 254 nm. The column chromatography purification of products was performed using silica gel (0.06-0.2 nm, Sigma) as stationary phase and a mixture of *n*-hexane/ethyl acetate as eluent. The corresponding ^{1}H-NMR and ^{13}C-NMR spectra of starting materials and products were recorded at 300 MHz (Bruker ARX-300) or 400 MHz (Bruker AV400) using deuterated DMSO as solvent. Chemical shifts are provided in the δ scale relative to residual DMSO (2.50 ppm) for ^{1}H-NMR spectra and to the central line of DMSO-d_6 (39.43 ppm) for ^{13}C-NMR (APT) spectra. Chiral HPLC analysis was performed in a Waters 600 equipment with Daicel Chiralpak IA and IC columns, employing mixtures of *n*-hexane/ethyl acetate and *n*-hexane/tetrahydrofuran as eluent. The specific rotation of products was recorded in $CHCl_3$ or acetone using a Jasco P-1020 polarimeter. Melting point determination was carried out in a Gallenkamp MPD 350 BM 2.5 apparatus. Infrared spectra of starting materials and products were recorded by employment of attenuated total reflection infrared (ATR-IR) equipment (PerkinElmer Spectrum 100 FT-IR). The HRMS analysis was performed using a Q-TOF analyzer and ESI as ionization method (Bruker MicroTof-Q equipment). The synthesis of *N*-acylhydrazones **1a**,[30,31] **1e**,[30,31] **1f**,[30] **1l**,[30,31] and **1n**,[30] as well as catalysts **3c**[32] and **3d**,[33] was reached following the protocols described in literature. The spectroscopic data obtained of alkyl substituted *N*-acylhydrazones **1a**,[30,31] **1e**,[30,31] **1f**,[30] **1l**,[30,31] and **1n**,[30] catalysts **3c**[32] and **3d**,[34] and hydrazide derivative **4na**[6] are consistent with the values previously reported in literature. DFT calculations were performed by using Gaussian 16;[22a] kinetic simulations to obtain concentration profiles were carried out with Berkeley Madonna.[24]

Synthesis of alkyl substituted *N*-acyl hydrazones 1.

(*E*)-*N´*-(2-Ethylidene)-4-nitrobenzohydrazide (1g)

An excess of acetaldehyde (2.0 mL, 35.8 mmol) is added to a solution of 4-nitrobenzoic acid hydrazide (2.59 g, 14.0 mmol) in dichloromethane (40 mL). The reaction mixture is stirred during one day at room temperature. After this time, the solvent is evaporated, and the residue is recrystallized in ethanol to afford 1.60 g of pale yellow solid (55% yield). The starting material **1g** is obtained as a mixture of isomers (*E*)/(*Z*) 90:10. M.p. 197-199 °C. IR (cm^{-1}) 3260 (N-H), 3080, 1651 (C=O), 1599, 1554 (N-H), 1518 (NO_2), 1487, 1380, 1340 (NO_2), 1302, 1281, 868, 843, 718. ^{1}H-NMR (400 MHz, DMSO-d_6) δ 1.95 (d, *J* = 7.2 Hz, 3H, RCH_3), 7.77 (q, *J* = 7.2 Hz, 1H, N=CHR), 8.08 (d, *J* = 11.6 Hz, 2H, Ar-H), 8.34 (d, *J* = 11.6 Hz, 2H, Ar-H), 11.72 (s, 1H, N-H). ^{13}C-NMR (100.6 MHz, DMSO-d_6) δ 18.4 (CH_3), 123.5 (2 x C_{Ar}-H), 129.0 (2 x C_{Ar}-H), 139.3 (C_{Ar}), 149.1 (C_{Ar}), 149.8 (N=CHR), 161.0 (C=O). HRMS (ESI+) calcd for $[NaC_9H_9N_3O_3]^+$ 230.0536; found 230.0534 $[M + Na]^+$.

(*E*)-*N´*-(2-Ethylidene)-4-chlorobenzohydrazide (1h)

An excess of acetaldehyde (0.85 mL, 15.1 mmol) is added to a solution of 4-chlorobenzoic acid hydrazide (0.87 g, 5.0 mmol) in dichloromethane (5 mL). The reaction mixture is stirred during one day at room temperature. After this time, the solvent is evaporated and the residue is recrystallized in ethanol to afford 0.42 g of a white solid (42% yield). The starting material **1h** is obtained as a mixture of isomers (*E*)/(*Z*) 93:7. M.p. 180-182 °C. IR (cm^{-1}) 3204 (N-H), 3061, 2914, 1647 (C=O), 1621, 1594, 1546 (N-H), 1485, 1400, 1352, 1297, 1275, 868, 842, 528. ^{1}H-NMR (400 MHz, DMSO-d_6) δ 1.93 (d, *J* = 5.6 Hz, 3H, RCH_3), 7.57 (d, *J* = 8.4 Hz, 2H,

Ar-H), 7.74 (q, *J* = 5.2 Hz, 1H, N=CHR), 7.86 (d, *J* = 8.4 Hz, 2H, Ar-H), 11.50 (s, 1H, N-H). ^{13}C-NMR (100.6 MHz, DMSO-d_6) δ 18.4 (CH_3), 128.5 (2 x C_{Ar}-H), 129.4 (2 x C_{Ar}-H), 132.3 (C_{Ar}), 136.3 (C_{Ar}), 148.9 (N=CHR), 161.6 (C=O). HRMS (ESI+) calcd for $[NaC_9H_9ClN_2O]^+$ 219.0296; found 219.0306 $[M + Na]^+$.

(*E*)-*N´*-(2-Ethylidene)-4-bromobenzohydrazide (1i)

An excess of acetaldehyde (0.85 mL, 15.1 mmol) is added to a solution of 4-bromobenzoic acid hydrazide (1.10 g, 5.0 mmol) in dichloromethane (5 mL). The reaction mixture is stirred during one day at room temperature. After this time, the solvent is evaporated, and the residue is recrystallized in ethanol to afford 0.68 g of white solid (56% yield). The starting material **1i** is obtained as a mixture of isomers (*E*)/(*Z*) 93:7. M.p. 189-191 °C. IR (cm^{-1}) 3187 (N-H), 3060, 2833, 1650 (C=O), 1621, 1591, 1552 (N-H), 1484, 1395, 1354, 1300, 1283, 1269, 868, 837, 504. ^{1}H-NMR (400 MHz, DMSO-d_6) δ 1.93 (d, *J* = 5.2 Hz, 3H, -CH_3), 7.70-7.80 (m, 5H, Ar-H + N=CHR), 11.50 (s, 1H, N-H). ^{13}C-NMR (100.6 MHz, DMSO-d_6) δ 18.4 (CH_3), 125.2 (C_{Ar}), 129.6 (2 x C_{Ar}-H), 131.4 (2 x C_{Ar}-H), 132.6 (C_{Ar}), 148.9 (N=CHR), 161.8 (C=O). HRMS (ESI+) calcd for $[NaC_9H_9BrN_2O]^+$ 262.9790; found 262.9805 $[M + Na]^+$.

(*E*)-*N´*-(2-Propylidene)-4-nitrobenzohydrazide (1j)

An excess of propionaldehyde (0.44 mL, 6.0 mmol) is added to a solution of 4-nitrobenzoic acid hydrazide (0.92 g, 5.0 mmol) in dichloromethane (10 mL). The reaction mixture is stirred during one day at room temperature. After this time, the solvent is evaporated, and the residue is recrystallized in ethanol to afford 0.52 g of a pale yellow solid (47% yield. The starting material **1j** is obtained as a mixture of isomers (*E*)/(*Z*) 91:9. M.p. 160-162 °C. IR (cm^{-1}) 3212 (N-H), 3055, 2973, 1651 (C=O), 1600, 1557 (N-H), 1516 (NO_2), 1489, 1341 (NO_2), 1325, 1302, 1279, 868, 847, 707. ^{1}H-NMR (300 MHz, DMSO-d_6) δ 1.06 (t, *J* = 7.5 Hz, 3H, RCH_3), 2.30 (dq, J^1 = 5.1 Hz, J^2 = 7.5 Hz, 2H, RCH_2R'), 7.78 (t, *J* = 5.1 Hz, 1H, N=CHR), 8.06-8.09 (m, 2H, Ar-H), 8.32-8.35 (m, 2H, Ar-H), 11.70 (s, 1H, N-H). ^{13}C-NMR (75 MHz, DMSO-d_6) δ 10.5 (CH_3), 25.5 (CH_2) 123.6 (2 x C_{Ar}-H), 129.1 (2 x C_{Ar}-H), 139.3 (C_{Ar}), 149.1 (C_{Ar}), 154.5 (N=CHR), 161.2 (C=O). HRMS (ESI+) calcd for $[NaC_{10}H_{11}N_3O_3]^+$ 244.0693; found 244.0712 $[M + Na]^+$.

(*E*)-*N´*-(2-Heptylidene)-4-nitrobenzohydrazide (1k)

An excess of heptaldehyde (0.86 mL, 6.0 mmol) is added to a solution of 4-nitrobenzoic acid hydrazide (0.92 g, 5.0 mmol) in dichloromethane (10 mL). The reaction mixture is stirred during one day at room temperature. After this time, the solvent is evaporated and the residue is recrystallized in ethanol to afford 1.02 g of a pale yellow solid (74% yield). The starting material **1k** is obtained as a mixture of isomers (*E*)/(*Z*) 90:10. M.p. 106-108 °C. IR (cm^{-1}) 3244 (N-H), 3073, 2938, 1660 (C=O), 1599, 1552 (N-H), 1513 (NO_2), 1348 (NO_2), 1318, 1288, 867, 845, 693. ^{1}H-NMR (400 MHz, DMSO-d_6) δ 0.85-0.89 (m, 3H, RCH_3), 1.23-1.36 (m, 6H, RCH_2R'), 1.46-1.53 (m, 2H, RCH_2R'), 2.25-2.30 (m, 2H, RCH_2R'), 7.76 (t, *J* = 5.2 Hz, 1H, N=CHR), 8.07-8.09 (m, 2H, Ar-H), 8.33-8.35 (m, 2H, Ar-H), 11.70 (s, 1H, N-H). ^{13}C-NMR (100.6 MHz, DMSO-d_6) δ 13.9 (CH_3), 22.0 (CH_2), 25.9 (CH_2), 28.3 (CH_2), 31.1 (CH_2), 32.0 (CH_2), 123.6 (2 x C_{Ar}-H), 129.0 (2 x C_{Ar}-H), 139.3 (C_{Ar}), 149.1 (C_{Ar}), 153.7 (N=CHR), 161.1 (C=O). HRMS (ESI+) calcd for $[NaC_{14}H_{19}N_3O_3]^+$ 300.1319; found 300.1309 $[M + Na]^+$.

(*E*)-*N´*-(2-Benzylmethylidene)-4-nitrobenzohydrazide (1m)

An excess of phenylacetaldehyde (0.59 mL, 4.8 mmol) is added to a solution of 4-nitrobenzoic acid hydrazide (0.74 g, 4.0 mmol) in dichloromethane (15 mL). The reaction mixture is stirred during one day at room temperature. After this time, the solvent is evaporated and the residue is recrystallized in ethanol to afford 0.78 g of a yellow solid (68% yield). The starting material **1m** is obtained as a mixture of isomers (*E*)/(*Z*) 90:10. M.p. 158-160 °C. IR (cm^{-1}) 3179 (N-H), 3046, 1654 (C=O), 1599, 1542 (N-H), 1513 (NO_2), 1347 (NO_2), 1284, 860, 845, 695. ^{1}H-NMR (300 MHz, DMSO-d_6) δ 3.65 (d, *J* = 6.0 Hz, 2H, RCH_2R'), 7.23-7.38 (m, 5H, Ar-H), 7.87 (t, *J* = 6.0 Hz, 1H, N=CHR), 8.09 (d, *J* = 8.9 Hz, 2H, Ar-H), 8.34 (d, *J* = 8.8 Hz, 2H, Ar-H), 11.81 (s, 1H, N-H). ^{13}C-NMR (75 MHz, DMSO-d_6) δ 38.4 (CH_2), 123.6 (2 x C_{Ar}-H), 126.7 (C_{Ar}-H), 128.7 (2 x C_{Ar}-H), 128.9 (2 x C_{Ar}-H), 129.1 (2 x C_{Ar}-H), 136.7 (C_{Ar}), 139.1 (C_{Ar}), 149.2 (C_{Ar}), 152.0 (N=CHR), 161.3 (C=O). HRMS (ESI+) calcd for $[NaC_{15}H_{13}N_3O_3]^+$ 306.0849; found 306.0870 $[M + Na]^+$.

General procedure for the enantioselective synthesis of hydrazide derivatives 4.

The corresponding nitroalkane **2** (1 mL) is added to a mixture of *N*-acylhydrazone **1** (0.1 mmol) and catalyst **3a** (0.03 mmol, 9.73 mg) in a test tube. The reaction mixture is stirred at the indicated temperature and the formation of corresponding products is followed by TLC. After the time described below, the residue is purified by column chromatography using a mixture of *n*-hexane/ethyl acetate to afford the pure adducts **4**. Diastereomeric ratio (dr) is determined by ^{1}H-NMR spectroscopy analysis from an aliquot of the reaction mixture after the time described, using DMSO-d_6 as solvent. Enantiomeric excesses (ee) of isolated products are obtained via chiral HPLC analysis using mixtures of *n*-hexane/ethyl acetate and *n*-hexane/tetrahydrofuran as eluent. The reaction conditions as well as yield and selectivity of distinct products are collected in Table 1.

(*S*)-*N'*-(3-Methyl-1-nitrobutan-2-yl)-4-nitrobenzohydrazide (4aa)

From hydrazone **1a** (23.52 mg, 0.1 mmol) and nitromethane (**2a**) (1 mL, 18.3 mmol), after three days at room temperature, compound **4aa** was purified by column chromatography in *n*-hexane-ethyl acetate 8:2 to afford 16.89 mg of yellow oil (57% yield). The corresponding ee (40%) was determined by HPLC using a Daicel Chiralpak IC column (*n*-hexane/ethyl acetate 85:15, flow rate 1 mL·min^{-1}, λ = 347.9 nm): τmajor = 19.7 min; τminor = 22.7 min. $[\alpha]_D^{24.2}$ = -1.82 (*c* 1.17, acetone, 40% ee). IR (cm^{-1}) 3285 (N-H), 3106, 2958, 1648 (C=O), 1599, 1550 (N-H), 1523 (NO_2), 1461, 1376, 1344 (NO_2), 867, 849, 714. ^{1}H-NMR (300 MHz, DMSO-d_6) δ 0.97 (dd, J^1 = 7.1 Hz, J^2 = 0.8 Hz, 6H, RCH_3), 1.87-1.98 (m, 1H, R'CHR_2), 3.54 (dq, J^1 = 4.0 Hz, J^2 = 1.2 Hz, 1H, NCHRR'), 4.54 (dd, J^1 = 13.6 Hz, J^2 = 7.9 Hz, 1H, RCH_2NO_2), 4.72 (dd, J^1 = 13.6 Hz, J^2 = 3.9 Hz, 1H, RCH_2NO_2), 5.48 (t, *J* = 5.9 Hz, 1H, N-NH-C), 7.97-8.01 (m, 2H, Ar-H), 8.29-8.31 (m, 2H, Ar-H), 10.32 (d, *J* = 6.2 Hz, 1H, (RC=O)NHR). ^{13}C-NMR (75 MHz, DMSO-d_6) δ 18.1 (CH_3), 19.0 (CH_3), 28.8 (CH), 63.2 (NCHRR'), 76.9 (RCH_2NO_2), 124.0 (2 x C_{Ar}-H), 129.1 (2 x C_{Ar}-H), 139.0 (C_{Ar}), 149.6 (C_{Ar}), 164.7 (C=O). HRMS (ESI+) calcd for $[NaC_{12}H_{16}N_4O_5]^+$ 319.1013; found 319.1017 $[M + Na]^+$.

(*S*)-4-Nitro-*N'*-(1-nitropropan-2-yl)benzohydrazide (4ga)

From hydrazone **1g** (20.72 mg, 0.1 mmol) and nitromethane (**2a**) (1 mL, 18.3 mmol), after three days at room temperature, compound **4ga** was purified by column chromatography in *n*-hexane-ethyl acetate 6:4 to afford 24.50 mg of yellow solid (91% yield). The corresponding ee (42%) was determined by HPLC using a Daicel Chiralpak IC column (*n*-hexane/ethyl acetate 85:15, flow rate 1 mL·min^{-1}, λ = 325.2 nm): τmajor = 19.4 min; τminor = 20.8 min. $[\alpha]_D^{28.5}$ = -1.91 (*c* 1.23, acetone, 45% ee). M.p. 112-114 °C. IR (cm^{-1}) 3352 (N-H), 3313 (N-H), 3110, 2977, 1665 (C=O), 1597, 1555 (N-H), 1516 (NO_2), 1409, 1379, 1343 (NO_2), 1324, 1305, 866, 844, 712. ^{1}H-NMR (300 MHz, DMSO-d_6) δ 1.12 (d, *J* = 6.6 Hz, 3H, RCH_3), 3.81-3.85 (m, 1H, NCHRR'), 4.56 (dd, J^1 = 13.0 Hz, J^2 = 5.4 Hz, 1H, RCH_2NO_2), 4.65 (dd, J^1 = 13.0 Hz, J^2 = 7.2 Hz, 1H, RCH_2NO_2), 5.49-5.61 (m, 1H, N-NH-C), 8.04 (d, *J* = 9.0 Hz, 2H, Ar-H), 8.32 (d, *J* = 9.0 Hz, 2H, Ar-H), 10.32 (d, *J* = 6.4 Hz, 1H, (RC=O)NHR). ^{13}C-NMR (75 MHz, DMSO-d_6) δ 15.9 (CH_3), 53.4 (NCHRR'), 79.0 (RCH_2NO_2), 123.5 (2 x C_{Ar}-H), 128.7 (2 x C_{Ar}-H), 138.6 (C_{Ar}), 149.1 (C_{Ar}), 164.3 (C=O). HRMS (ESI+) calcd for $[NaC_{10}H_{12}N_4O_5]^+$ 291.0700; found 291.0709 $[M + Na]^+$.

(*S*)-4-Chloro-*N'*-(1-nitropropan-2-yl)benzohydrazide (4ha)

From hydrazone **1h** (19.63 mg, 0.1 mmol) and nitromethane (**2a**) (1 mL, 18.3 mmol), after three days at room temperature, compound **4ha** was purified by column chromatography in *n*-hexane/ethyl acetate 7:3 to afford 14.17 mg of pale yellow solid (55% yield). The corresponding ee (37%) was determined by HPLC using a Daicel Chiralpak IA column (*n*-hexane/ethyl acetate 70:30, flow rate 1 mL·min^{-1}, λ = 247.2 nm): τmajor = 19.5 min; τminor = 18.0 min. $[\alpha]_D^{27.8}$ = -3.68 (*c* 0.72, acetone, 37% ee). M.p. 114-116 °C. IR (cm^{-1}) 3277 (N-H), 2982, 1623 (C=O), 1596, 1542 (N-H), 1459, 1444, 1389, 1306, 1092, 839, 802, 527. ^{1}H-NMR (300 MHz, DMSO-d_6) δ 1.11 (d, *J* = 6.6 Hz, 3H, RCH_3), 3.63-3.76 (m, 1H, NCHRR'), 4.53 (dd, J^1 = 13.2 Hz, J^2 = 5.4 Hz, 1H, RCH_2NO_2), 4.62 (dd, J^1 = 13.2 Hz, J^2 = 7.2 Hz, 1H, RCH_2NO_2), 5.43 (t, *J* = 6.3 Hz, 1H, N-NH-C), 7.52-7.56 (m, 2H, Ar-H), 7.80-7.85 (m, 2H, Ar-H), 10.06 (d, *J* = 6.3 Hz, 1H, (RC=O)NHR). ^{13}C-NMR (75 MHz, DMSO-d_6) δ 15.9 (CH_3), 53.5 (NCHRR'), 79.1 (RCH_2NO_2), 128.4 (2 x C_{Ar}-H), 129.1 (2 x C_{Ar}-H), 131.6 (C_{Ar}), 136.2 (C_{Ar}), 165.1 (C=O). HRMS (ESI+) calcd for $[NaC_{10}H_{12}ClN_3O_3]^+$ 280.0459; found 280.0433 [M + Na]$^+$.

(*S*)-4-Bromo-*N*′-(1-nitropropan-2-yl)benzohydrazide (4ia)

From hydrazone **1i** (24.11 mg, 0.1 mmol) and nitromethane (**2a**) (1 mL, 18.3 mmol), after three days at room temperature, compound **4ia** was purified by column chromatography in *n*-hexane/ethyl acetate 7:3 to afford 7.25 mg of white solid (24% yield). The corresponding ee (39%) was determined by HPLC using a Daicel Chiralpak IA column (*n*-hexane/ethyl acetate 70:30, flow rate 1 mL·min^{-1}, λ = 246.0 nm): τmajor = 23.5 min; τminor = 20.0 min. $[\alpha]_D^{27.9}$ = -5.07 (*c* 0.36, acetone, 39% ee). M.p. 121-123 °C. IR (cm^{-1}) 3275 (N-H), 3095, 2975, 1623 (C=O), 1591, 1544 (N-H), 1459, 1444, 1389, 1302, 1071, 837, 801, 503. ^{1}H-NMR (300 MHz, DMSO-d_6) δ 1.11 (d, *J* = 6.6 Hz, 3H, RCH_3), 3.63-3.76 (m, 1H, NCHRR'), 4.53 (dd, J^1 = 12.9 Hz, J^2 = 5.1 Hz, 1H, RCH_2NO_2), 4.62 (dd, J^1 = 12.9 Hz, J^2 = 6.9 Hz, 1H, RCH_2NO_2), 5.40-5.45 (m, 1H, N-NH-C), 7.66-7.70 (m, 2H, Ar-H), 7.73-7.77 (m, 2H, Ar-H), 10.06 (d, *J* = 6.3 Hz, 1H, (RC=O)NHR). ^{13}C-NMR (75 MHz, DMSO-d_6) δ 15.9 (CH_3), 53.5 (NCHRR'), 79.1 (RCH_2NO_2), 125.1 (C_{Ar}), 129.3 (2 x C_{Ar}-H), 131.3 (2 x C_{Ar}-H), 132.0 (C_{Ar}), 165.2 (C=O). HRMS (ESI+) calcd for $[NaC_{10}H_{12}BrN_3O_3]^+$ 323.9954; found 323.9943 [M + Na]$^+$.

(*S*)-4-Nitro-*N*′-(1-nitrobutan-2-yl)benzohydrazide (4ja)

From hydrazone **1j** (24.11 mg, 0.1 mmol) and nitromethane (**2a**) (1 mL, 18.3 mmol), after three days at room temperature, compound **4ja** was isolate by column chromatography in *n*-hexane/ethyl acetate 7:3 to afford 22.3 mg of yellow solid (79% yield). The corresponding ee (39%) was determined by HPLC using a Daicel Chiralpak IC column (*n*-hexane/ethyl acetate 85:15, flow rate 1 mL·min-1, λ = 255.5 nm): τmajor = 17.4 min; τminor = 19.2 min. $[\alpha]_D^{29.5}$ = -6.91 (*c* 1.11, acetone, 39% ee). M.p. 135-137 °C. IR (cm^{-1}) 3271 (N-H), 3107, 2934, 1625 (C=O), 1595, 1551 (N-H), 1511 (NO_2), 1424, 1395, 1346 (NO_2), 1326, 1315, 868, 849, 714. ^{1}H-NMR (300 MHz, DMSO-d_6) δ 0.97 (t, *J* = 7.5 Hz, 3H, RCH_3), 1.39-166 (m, 2H, RCH_2R'), 3.48-3.59 (m, 1H, NCHRR'), 4.59-4.66 (m, 2H, RCH_2NO_2), 5.52 (t, *J* = 6.0 Hz, 1H, N-NH-C), 8.00-8.05 (m, 2H, Ar-H), 8.29-8.33 (m, 2H, Ar-H), 10.30 (d, *J* = 6.3 Hz, 1H, (RC=O)NHR). ^{13}C-NMR (75 MHz, DMSO-d_6) δ 10.1 (CH_3), 22.9 (CH_2), 59.2 (NCHRR'), 77.6 (RCH_2NO_2), 123.5 (2 x C_{Ar}-H), 128.7 (2 x C_{Ar}-H), 138.6 (C_{Ar}), 149.1 (C_{Ar}), 164.3 (C=O). HRMS (ESI+) calcd for $[NaC_{11}H_{14}N_4O_5]^+$ 305.0856; found 305.0850 [M + Na]$^+$.

(*S*)-4-Nitro-*N*′-(1-nitrooctan-2-yl)benzohydrazide (4ka)

From hydrazone **1k** (27.73 mg, 0.1 mmol) and nitromethane (**2a**) (1 mL, 18.3 mmol), after three days at room temperature, compound **4ka** was purified by column chromatography in *n*-hexane/ethyl acetate 8:2 to afford 26.73 mg of yellow solid (79% yield). The corresponding ee (39%) was determined by HPLC using a Daicel Chiralpak IC column (*n*-hexane/ethyl acetate 85:15, flow rate 1 mL·min^{-1}, λ = 255.5 nm): τmajor = 12.5 min; τminor = 14.2 min. $[\alpha]_D^{29.6}$ = -4.92 (*c* 1.34, acetone, 39% ee). M.p. 96-98 °C. IR (cm^{-1}) 3391 (N-H), 3311 (N-H), 3108, 2952, 1661 (C=O), 1598, 1549 (N-H), 1517 (NO_2), 1462, 1383, 1339 (NO_2), 1327, 872, 846, 713. ^{1}H-NMR (300 MHz, DMSO-d_6) δ 0.80-0.91 (m, 3H, RCH_3), 1.17-1.36 (m, 6H, Alk-H), 1.35-1.49 (m, 3H, Alk-H), 1.49-1.60 (m, 1H, Alk-H), 3.56-3.63 (m, 1H, NCHRR'), 4.61 (d, *J* = 6.0 Hz, 2H, RCH_2NO_2), 5.51 (t, *J* = 5.9 Hz, 1H, N-NH-C), 8.00-8.04 (m, 2H, Ar-H), 8.29-8.34 (m, 2H, Ar-H), 10.30 (d, *J* = 6.5 Hz, 1H, (RC=O)NHR). ^{13}C-NMR (75 MHz, DMSO-d_6) δ 14.0 (CH_3), 22.0 (CH_2), 25.1 (CH_2), 28.6 (CH_2), 29.8 (CH_2), 31.1 (CH_2), 57.8 (NCHRR'), 78.0 (RCH_2NO_2), 123.5 (2 x C_{Ar}-H), 128.7 (2 x C_{Ar}-H), 138.6 (C_{Ar}), 149.1 (C_{Ar}), 164.2 (C=O). HRMS (ESI+) calcd for $[NaC_{15}H_{22}N_4O_5]^+$ 361.1482; found 361.1479 [M + Na]$^+$.

(*S*)-*N*′-(3-Methyl-1-nitropentan-2-yl)-4-nitrobenzohydrazide (4la)

From hydrazone **1l** (24.93 mg, 0.1 mmol) and nitromethane (**2a**) (1 mL, 18.3 mmol), after three days at room temperature, compound **4la** was purified by column chromatography in *n*-hexane/ethyl acetate 8:2 to afford 25.87 mg of yellow solid (83% yield). The corresponding ee (40%) was determined by HPLC using a Daicel Chiralpak IC column (*n*-hexane/ethyl acetate 85:15, flow rate 1 mL·min^{-1}, λ = 255.5 nm): τmajor = 12.4 min; τminor = 17.7 min. $[\alpha]_D^{29.1}$ = -8.20 (*c* 1.29, acetone, 40% ee). M.p. 118-120 °C. IR (cm^{-1}) 3379 (N-H), 3301 (N-H), 3108, 2953, 1657 (C=O), 1596, 1550 (N-H), 1513 (NO_2), 1467, 1383, 1345 (NO_2), 1320, 867, 845, 714. ^{1}H-NMR (300 MHz, DMSO-d_6) δ 0.90 (t, *J* = 6.6 Hz, 6H, RCH_3), 1.20 (ddd, J^1 = 13.8 Hz, J^2 = 7.7 Hz, J^3 = 5.1 Hz, 1H, RCH_2R'), 1.46 (ddd, J^1 = 14.0 Hz, J^2 = 7.7 Hz, J^3 = 6.5 Hz, 1H, RCH_2R'), 1.74-1.90 (m, 1H, R_2CHR'), 3.61-3.71 (m, 1H, NCHRR'), 4.54-4.66 (m, 2H, RCH_2NO_2), 5.50 (t, *J* = 6.0 Hz, 1H, N-NH-C), 8.00-8.04 (m, 2H, Ar-H), 8.30-8.34 (m, 2H, Ar-H), 10.31 (d, *J* = 6.5 Hz, 1H, (RC=O)NHR). ^{13}C-NMR (75 MHz, DMSO-d_6) δ 22.2 (CH_3), 22.8 (CH_3), 24.0 (CH), 39.0 (CH_2), 56.1 (NCHRR'), 78.3 (RCH_2NO_2), 123.6 (2 x C_{Ar}-H), 128.7 (2 x C_{Ar}-H), 138.6 (C_{Ar}), 149.1 (C_{Ar}), 164.3 (C=O). HRMS (ESI+) calcd for $[NaC_{13}H_{18}N_4O_5]^+$ 333.1169; found 333.1167 [M + Na]$^+$.

(*S*)-4-Nitro-*N*′-(1-nitro-3-phenylpropan-2-yl)benzohydrazide (4ma)

From hydrazone **1m** (28.33 mg, 0.1 mmol) and nitromethane (**2a**) (1 mL, 18.3 mmol), after three days at room temperature, compound **4ma** was purified by column chromatography in *n*-hexane/ethyl acetate 7:3 to afford 25.47 mg of yellow solid (74% yield). The corresponding ee (43%) was determined by HPLC using a Daicel Chiralpak IC column (*n*-hexane/ethyl acetate 85:15, flow rate 1 mL·min^{-1}, λ = 256.7 nm): τmajor = 16.1 min; τminor = 18.2 min. $[\alpha]_D^{24.5}$ = -5.73 (*c* 1.27, acetone, 43% ee). M.p. 153-155 °C. IR (cm^{-1}) 3281 (N-H), 3200 (N-H), 3106, 2926, 1670 (C=O), 1649, 1597, 1548 (N-H), 1528 (NO_2), 1448, 1388, 1346 (NO_2), 1319, 864, 849, 707. ^{1}H-NMR (75 MHz, DMSO-d_6) δ 2.74 (dd, J^1 = 14.0 Hz, J^2 = 7.4 Hz, 1H, RCH_2Ph), 2.95 (dd, J^1 = 13.9 Hz, J^2 = 6.3 Hz, 1H, RCH_2Ph), 3.85-3.96 (m, 1H, NCHRR'), 4.51 (dd, J^1 = 13.4 Hz, J^2 = 4.5 Hz, 1H, RCH_2NO_2), 4.64 (dd, J^1 = 13.4 Hz, J^2 = 7.7 Hz, 1H, RCH_2NO_2), 5.67 (t, *J* = 6.4 Hz, 1H, N-NH-C), 7.19-7.36 (m, 5H, Ar-H), 7.99-8.03 (m, 2H, Ar-H), 8.28-8.33 (m, 2H, Ar-H), 10.39 (d, *J* = 6.5 Hz, 1H, (RC=O)NHR). ^{13}C-NMR (75 MHz, DMSO-d_6) δ 36.2 (CH_2), 59.4 (NCHRR'), 77.2 (RCH_2NO_2), 123.5 (2 x C_{Ar}-H), 126.5 (C_{Ar}-H), 128.4 (2 x C_{Ar}-H), 128.7 (2 x C_{Ar}-H), 129.3 (2 x C_{Ar}-H), 137.6 (C_{Ar}), 138.5 (C_{Ar}), 149.1 (C_{Ar}), 164.2 (C=O). HRMS (ESI+) calcd for $[NaC_{16}H_{16}N_4O_5]^+$ 367.1013; found 367.1020 [M + Na]$^+$.

(*S*)-4-Nitro-*N*′-(1-nitro-4-phenylbutan-2-yl)benzohydrazide (4na)[6]

From hydrazone **1n** (29.73 mg, 0.1 mmol) and nitromethane (**2a**) (1 mL, 18.3 mmol), after three days at room temperature, compound **4na** was purified by column chromatography in *n*-hexane/ethyl acetate 8:2 to afford 28.67 mg of yellow solid (80% yield). The corresponding ee (41%) was determined by HPLC using a Daicel Chiralpak IC column (*n*-hexane/ethyl acetate 85:15, flow rate 1 mL·min^{-1}, λ = 256.7 nm): τmajor =

15.5 min; τminor = 17.8 min. $[\alpha]_D^{27.7}$ = -7.29 (*c* 1.43, acetone, 41% ee). {lit.[6] $[\alpha]_D^{25}$ = -10.5 (*c* 0.31, acetone) for (*S*)-**4na**, 26% ee}.

4-Nitro-*N'*-(3-nitrobutan-2-yl)benzohydrazide (4gb)

From hydrazone **1g** (20.72 mg, 0.1 mmol) and nitroethane (**2b**) (1 mL 12.6 mmol), after seven days at -20 °C, compound **4gb** was purified by column chromatography in *n*-hexane/ethyl acetate 7:3 to afford 18.46 mg of a mixture of diastereomers (1.4:1 d.r.) as a yellow solid (65% yield). The corresponding ee (54%) was determined respect to the major diastereomer by HPLC using a Daicel Chiralpak IC column (n-hexane/tetrahydrofuran 90:10, flow rate 1 mL·min^{-1}, λ = 241.7 nm): τmajor = 27.0 min; τminor = 36.5 min. M.p. 111-113 °C. IR (cm^{-1}) 3242 (N-H), 3092, 2988, 1640 (C=O), 1598, 1541 (N-H), 1522 (NO_2), 1451, 1392, 1344 (NO_2), 1321, 1307, 871, 849, 690. ^{1}H-NMR (300 MHz, DMSO-d_6) δ 1.04 (d, *J* = 6.6 Hz, 3H$_a$, RCH$_3$), 1.09 (d, *J* = 6.7 Hz, 3H$_b$, RCH$_3$), 1.46 (d, *J* = 6.7 Hz, 3H$_a$, RCH$_3$), 1.51 (d, *J* = 6.7 Hz, 3H$_b$, RCH$_3$), 3.51-3.66 (m, 1H$_a$ + 1H$_b$, NCHRR'), 4.73-4.86 (m, 1H$_a$ + 1H$_b$, RCHR'NO$_2$), 5.39 (dd, J^1 = 5.5 Hz, J^2 = 4.5 Hz, 1H$_b$, N-NH-C), 5.49 (t, *J* = 6.0 Hz, 1H$_a$, N-NH-C), 7.98-8.07 (m, 2H$_a$+2H$_b$, Ar-H), 8.29-8.34 (m, 2H$_a$+2H$_b$, Ar-H), 10.20 (d, *J* = 5.6 Hz, 1H$_b$, (RC=O)NHR), 10.33 (d, *J* = 6.3 Hz, 1H$_a$, (RC=O)NHR). ^{13}C-NMR (75 MHz, DMSO-d_6) δ 13.5 (CH$_3$), 13.9 (CH$_3$), 14.1 (CH$_3$), 14.8 (CH$_3$), 57.3 (NCHRR'), 57.8 (NCHRR'), 85.0 (RCHR'NO$_2$), 85.1 (RCHR'NO$_2$), 123.6 (2 x C$_{Ar}$-H), 123.6 (2 x C$_{Ar}$-H), 128.7 (2 x C$_{Ar}$-H(a) + 2 x C$_{Ar}$-H(b)), 138.6 (C$_{Ar}$), 138.7 (C$_{Ar}$), 149.1 (C$_{Ar}$(a) + C$_{Ar}$(b)), 164.1 (C=O), 164.6 (C=O). HRMS (ESI+) calcd for $[NaC_{11}H_{14}N_4O_5]^+$ 305.0856; found 305.0869 $[M + Na]^+$.

4-Nitro-*N'*-(2-nitropentan-3-yl)benzohydrazide (4jb)

From hydrazone **1j** (24.11 mg, 0.1 mmol) and nitroethane (**2b**) (1 mL, 12.6 mmol), after seven days at -20 °C, compound **4jb** was purified by column chromatography in *n*-hexane/ethyl acetate 7:3 to afford 11.72 mg of a mixture of diastereomers (1.7:1 dr) as a yellow solid (40% yield). The corresponding ee (50%) was determined by HPLC using a Daicel Chiralpak IC column (*n*-hexane/tetrahydrofuran 90:10, flow rate 1 mL·min^{-1}, λ = 256.7 nm): τmajor = 32.2 min; τminor = 25.5 min. M.p. 81-83 °C. IR (cm^{-1}) 3251 (N-H), 3082, 2968, 1627 (C=O), 1596, 1546 (N-H), 1519 (NO_2), 1448, 1390, 1338 (NO_2), 1318, 1302, 861, 847, 697. ^{1}H-NMR (300 MHz, DMSO-d_6) δ 0.96-1.04 (m, 3H$_a$ + 3H$_b$, RCH$_3$), 1.40-1.53 (m, 5H$_a$ + 5H$_b$, Alk-H), 3.56-3.37 (m, 1H$_a$ + 1H$_b$, NCHRR'), 4.72-4.88 (m, 1H$_a$ + 1H$_b$, RCHR'NO$_2$), 5.34 (dd, J^1 = 5.4 Hz, J^2 = 4.6 Hz, 1H$_b$, N-NH-C), 5.47 (t, *J* = 6.0 Hz, 1H$_a$, N-NH-C), 7.94-7.98 (m, 2H$_b$, Ar-H) 8.04-8.07 (m, 2H$_a$, Ar-H), 8.29-8.35 (m, 2H$_a$ + 2 H$_b$, Ar-H), 10.13 (d, *J* = 5.6 Hz, 1H$_b$, (RC=O)NHR), 10.36 (d, *J* = 6.3 Hz, 1H$_a$, (RC=O)NHR). ^{13}C-NMR (75 MHz, DMSO-d_6) δ 10.2 (CH$_3$), 10.8 (CH$_3$), 12.7 (CH$_3$), 13.7 (CH$_3$), 20.4 (CH$_2$), 22.5 (CH$_2$), 63.3 (NCHRR'), 63.7 (NCHRR'), 83.9 (RCHR'NO$_2$), 84.0 (RCHR'NO$_2$), 123.5 (2 x C$_{Ar}$-H), 123.6 (2 x C$_{Ar}$-H), 128.7 (2 x C$_{Ar}$-H), 128.7 (2 x C$_{Ar}$-H), 138.5 (C$_{Ar}$), 138.7 (C$_{Ar}$), 149.1 (C$_{Ar}$(a) + C$_{Ar}$(b)), 163.9 (C=O), 164.4 (C=O). HRMS (ESI+) calcd for $[NaC_{12}H_{16}N_4O_5]^+$ 319.1013; found 319.1020 $[M + Na]^+$.

4-Nitro-*N'*-(2-nitrononan-3-yl)benzohydrazide (4kb)

From hydrazone **1k** (27.73 mg, 0.1 mmol) and nitroethane (**2b**) (1 mL, 12.6 mmol), after seven days at -20 °C, compound **4kb** was purified by column chromatography in *n*-hexane/ethyl acetate 8:2 to afford 9.34 mg of a mixture of diastereomers (2.2:1 d.r.) as a yellow oil (27% yield). The corresponding ee (72%) was determined by HPLC using a Daicel Chiralpak IC column (*n*-hexane/tetrahydrofuran 90:10, flow rate 1 mL·min^{-1}, λ = 255.5 nm): τmajor = 24.7 min; τminor = 16.0 min. IR (cm^{-1}) 3282 (N-H), 2950, 2917, 1651 (C=O), 1600, 1547 (N-H), 1525 (NO_2), 1456, 1376, 1345 (NO_2), 1300, 867, 849, 718. ^{1}H-NMR (300 MHz, DMSO-d_6) δ 0.78-0.90 (m, 3H$_a$ + 3H$_b$, RCH$_3$), 0.97-1.60 (m, 13H$_a$ + 13H$_b$, Alk-H), 3.38-3.49 (m, 1H, NCHRR'), 3.54-3.65 (m, 1H, NCHRR'), 4.71-4.87 (m, 1H$_a$ + 1H$_b$, RCHR'NO$_2$), 5.30-5.34 (m, 1H$_b$, N-NH-C), 5.45 (t, *J* = 5.9 Hz, 1H$_a$, N-NH-C), 7.93-7.97 (m, 2H$_b$, Ar-H), 8.03-8.07 (m, 2H$_a$, Ar-H), 8.29-8.35 (m, 2H$_a$ + 2 H$_b$, Ar-H), 10.14 (d, *J* = 5.6 Hz, 1H$_b$, (RC=O)NHR), 10.37 (d, *J* = 6.3 Hz, 1H$_a$, (RC=O)NHR). ^{13}C-NMR (75 MHz, DMSO-d_6) δ 12.7 (CH$_3$), 13.3 (CH$_3$), 14.0 (CH$_3$), 22.1 (CH$_2$), 25.2 (CH$_2$), 25.7 (CH$_2$), 27.3 (CH$_2$), 28.6 (CH$_2$), 28.6 (CH$_2$), 29.4 (CH$_2$), 31.1 (CH$_2$), 31.1 (CH$_2$), 61.6 (NCHRR'), 62.2 (NCHRR'), 83.9 (RCHR'NO$_2$), 84.3 (RCHR'NO$_2$), 123.5 (2 x C$_{Ar}$-H), 123.6 (2 x C$_{Ar}$-H), 128.7 (2 x C$_{Ar}$-H), 128.7 (2 x C$_{Ar}$-H), 138.6 (C$_{Ar}$), 138.7 (C$_{Ar}$), 149.1 (C$_{Ar}$(a) + C$_{Ar}$(b)), 163.9 (C=O), 164.4 (C=O). HRMS (ESI+) calcd for $[NaC_{16}H_{24}N_4O_5]^+$ 375.1639; found 375.1645 $[M + Na]^+$.

***N'*-(4-Methyl-2-nitrohexan-3-yl)-4-nitrobenzohydrazide (4lb)**

From hydrazone **1l** (0.1 mmol, 24.93 mg, 0.1 mmol) and nitroethane (**2b**) (1 mL, 12.6 mmol), after seven days at -20 °C, compound **4lb** was purified by column chromatography in *n*-hexane/ethyl acetate 8:2 to afford 8.16 mg of a mixture of diastereomers (2.4:1 d.r.) as a pale yellow solid (25% yield). The corresponding ee (77%) was determined by HPLC using a Daicel Chiralpak IC column (*n*-hexane/tetrahydrofuran 90:10, flow rate 1 mL·min^{-1}, λ = 255.5 nm): τmajor = 27.8 min; τminor = 24.7 min. M.p. 132-134 °C. IR (cm^{-1}) 3263 (N-H), 2953, 2867, 1644 (C=O), 1599, 1548 (N-H), 1517 (NO_2), 1468, 1387, 1343 (NO_2), 1302, 870, 851, 718. ^{1}H-NMR (300 MHz, DMSO-d_6) δ 0.85-1.23 (m, 6H$_a$ + 6H$_b$, RCH$_3$), 1.31-1.43 (m, 4H, RCH$_2$R'), 1.46-1.51 (m, 3H$_a$ + 3H$_b$, RCH$_3$), 1.79-1-94 (m, 1H$_a$ + 1H$_b$, R$_2$CHR'), 3.48-3.56 (m, 1H, NCHRR'), 3.65-3.72 (m, 1H, NCHRR'), 4.69-4.77 (m, 1H, RCHR'NO$_2$), 4.81-4.89 (m, 1H, RCHR'NO$_2$), 5.28-5.31 (m, 1H, N-NH-C), 5.40-5.44 (m, 1H, N-NH-C), 7.93-7.97 (m, 2H, Ar-H), 8.04-8.08 (m, 2H, Ar-H), 8.29-8.35 (m, 2H$_a$ + 2H$_b$, Ar-H), 10.13 (d, *J* = 5.4 Hz, 1H, (RC=O)NHR), 10.37 (d, *J* = 6.3 Hz, 1H, (RC=O)NHR). ^{13}C-NMR (300 MHz, DMSO-d_6) δ 12.7 (C$_{Alk}$), 12.7 (C$_{Alk}$), 21.7 (C$_{Alk}$), 22.1 (C$_{Alk}$), 23.0 (C$_{Alk}$), 23.6 (C$_{Alk}$), 24.3 (C$_{Alk}$), 24.4 (C$_{Alk}$), 36.5 (CH$_2$), 38.6 (CH$_2$), 59.8 (NCHRR'), 60.5 (NCHRR'), 84.0 (RCHR'NO$_2$), 84.5 (RCHR'NO$_2$), 123.6 (2 x C$_{Ar}$-H), 123.7 (2 x C$_{Ar}$-H), 128.8 (2 x C$_{Ar}$-H), 128.8 (2 x C$_{Ar}$-H), 138.6 (C$_{Ar}$), 138.8 (C$_{Ar}$), 149.2 (C$_{Ar}$), 149.2 (C$_{Ar}$), 164.2 (C=O), 164.5 (C=O). Exact mass calculated for $[NaC_{14}H_{20}N_4O_5]^+$ $[M + Na]^+$ 347.1326; found 347.1321.

4-Nitro-*N'*-(4-nitro-1-phenylpentan-3-yl)benzohydrazide (4nb)

From hydrazone **1n** (29.73 mg, 0.1 mmol) and nitroethane (**2b**) (1 mL, 12.6 mmol), after seven days at -20 °C, compound **4nb** was purified by column chromatography in *n*-hexane/ethyl acetate 8:2 to afford 9.36 mg of a mixture of diastereomers (1.7:1 d.r.) as a yellow oil a yield of 41% (yellow oil). The corresponding ee (73%) was determined by HPLC using a Daicel Chiralpak IC column (*n*-hexane/ethyl acetate 85:15, flow rate 1 mL·min^{-1}, λ = 247.1 nm): τmajor = 14.1 min; τminor = 15.6 min. IR (cm^{-1}) 3284 (N-H), 2923, 1656 (C=O), 1600, 1544 (N-H), 1522 (NO_2), 1453, 1391, 1344 (NO_2), 1298, 866, 849, 699. ^{1}H-NMR (300 MHz, DMSO-d_6) δ 1.49-1.52 (m, 3H$_a$ + 3H$_b$, RCH$_3$), 1.59-1.79 (m, 2H$_a$ + 2H$_b$, RCH$_2$R'), 2.66-2.93 (m, 2H$_a$ + 2H$_b$, RCH$_2$R'), 3.42-3.50 (m, 1H, NCHRR'), 3.62-3.64 (m, 1H, NCHRR'), 4.79-4.93 (m, 1H$_a$ + 1H$_b$, RCHR'NO$_2$), 5.50-5.53 (m, 1H, N-NH-C), 5.67 (t, *J* = 6.0 Hz, 1H, N-NH-C), 7.16-7.31 (m, 5H$_a$ + 5H$_b$, Ar-H), 7.94-7.99 (m, 2H, Ar-H), 8.04-8.08 (m, 2H, Ar-H), 8.30-8.35 (m, 2H$_a$ + 2 H$_b$, Ar-H), 10.18 (d, *J* = 5.6 Hz, 1H, (RC=O)NHR), 10.41 (d, *J* = 6.3 Hz, 1H, (RC=O)NHR). ^{13}C-NMR (75 MHz, DMSO-d_6) δ 12.9 (CH$_3$), 13.7 (CH$_3$), 29.0 (CH$_2$), 29.6 (CH$_2$), 31.3 (CH$_2$), 31.5 (CH$_2$), 61.4 (NCHRR'), 62.0 (NCHRR'), 83.9 (RCHR'NO$_2$), 84.2 (RCHR'NO$_2$), 123.5 (2 x C$_{Ar}$-H), 123.6 (2 x C$_{Ar}$-H), 125.8 (C$_{Ar}$-H), 125.9 (C$_{Ar}$-H), 128.3 (2 x C$_{Ar}$-H(a) + 2 x C$_{Ar}$-H(b)), 128.4 (2 x C$_{Ar}$-H(a) + 2 x C$_{Ar}$-H(b)), 128.7 (2 x C$_{Ar}$-H), 128,8 (2 x C$_{Ar}$-H), 138.6 (C$_{Ar}$), 138.7 (C$_{Ar}$), 141.6 (C$_{Ar}$), 141.7 (C$_{Ar}$), 149.1 (C$_{Ar}$), 149.1 (C$_{Ar}$), 164.1 (C=O), 164.5 (C=O). HRMS (ESI+) calcd for $[NaC_{18}H_{20}N_4O_5]^+$ 395.1326; found 395.1329 $[M + Na]^+$.

General procedure for the calculation of initial rates.

A solution of mesitylene (0.25 M), as internal standard, in $CDCl_3$ (200 µl) is added to a mixture of hydrazone (**1h**, 0.05 or 0.025 mmol) and quinine (**3a**, 0.015 or 0.03 mmol) in a vial. The resulting mixture is stirred to form

a transparent colorless solution. The corresponding nitroalkane (5.5 mmol) is subsequently added and the new solution is transferred to an NMR tube after stirring. The concentration of hydrazone **1h** over reaction time is monitored by ^{1}H-NMR spectroscopy at 22.5 °C. Corresponding spectra are collected in a 300 MHz NMR spectrometer (Bruker, ARX-300), using the signal of mesitylene to calculate the concentration of reagent **1h** in the reaction medium. Initial rates are obtained from the slope of the straight lines resulting from interpolation of concentration *vs* time at the first moments of the reactions (Figure S70). A minimum of two replicas by experiment was performed, being the corresponding error the standard devia4agtion between distinct samples.

Acknowledgements

This work was supported by a 2018 Leonardo Grant for Researchers and Cultural Creators, BBVA Foundation. Authors thank Ministerio de Economía, Industria y Competitividad (MINECO/FEDER CTQ2016-75816-C2-1-P and CTQ2017-88091-P), Universidad de Zaragoza (JIUZ-2017-CIE-05) and Gobierno de Aragón-Fondo Social Europeo (E07_17R) for financial support of their research. All the calculations were performed in the Trueno cluster facility of SGAI-CSIC and the Extreme Science and Engineering Discovery Environment (XSEDE) through allocation TG-CHE190111. J.V.A.-R. thanks Dr. R. S. Paton for his help with the script to generate the PyMol style and GoodVibes.

Keywords: aza-Henry • hydrazone • nitroalkane • *β*-nitroalkylhydrazide • computational calculations

[1] a) B. Westermann, *Angew. Chem. Int. Ed.* **2003**, *42*, 151-153; b) A. Ting, S. E. Schaus, *Eur. J. Org. Chem.* **2007**, 5797-5815; c) E. Marqués-López, P. Merino, T. Tejero, R. P. Herrera, *Eur. J. Org. Chem.* **2009**, 2401-2420; d) A. Noble, J. C. Anderson, *Chem. Rev.* **2013**, *113*, 2887-2939; e) J. Kaur, P. Chauhan, S. Singh, S. S. Chimni, *Chem. Rec.* **2018**, *18*, 137-153.

[2] M. Sugiura, S. Kobayashi, *Angew. Chem. Int. Ed.* **2005**, *44*, 5176-5186.

[3] a) B. Narasimhan, P. Kumar, D. Sharma, *Acta Pharm. Sci.* **2010**, *52*, 169-180; b) R. Narang, B. Narasimhan, S. Sharma, *Curr. Med. Chem.* **2012**, *19*, 569-612.

[4] a) R. E. Carnahan, R. E. Kent, *US2865923*, **1958**; b) M. I. Vakulenko, L. V. Lapshina, S. I. Grishchenko, I. E. Efremova, V. M. Berestovitskaya, *Russ. J. Gen. Chem.* **2010**, *80*, 1930-1932; c) I. E. Efremova, M. I. Vakulenko, K. A. Lysenko, I. S. Bushmarinov, L. V. Lapshina, G. A. Berkova, V. M. Berestovitskaya, *Russ. J. Gen. Chem.* **2010**, *80*, 2298-2305; d) K. Fan, Y. Hui, X. Hu, H. Pang, Z. Xie, *New J. Chem.* **2015**, *39*, 5916-5919.

[5] a) E. J. Ariëns, *Eur. J. Clin. Pharmacol.* **1984**, *26*, 663-668; b) B. Waldeck, *Chirality* **1993**, *5*, 350-355; c) A. J. Hutt, S. C. Tan, *Drugs* **1996**, *52*, 1-12; d) M. C. Núñez, M. E. García-Rubiño, A. Conejo-García, O. Cruz-López, M. Kimatrai, M. A. Gallo, A. Espinosa, J. M. Campos, *Curr. Med. Chem.* **2009**, *16*, 2064-2074; e) W. H. Brooks, W. C. Guida, K. G. Daniel, *Curr. Top. Med. Chem.* **2011**, *11*, 760-770.

[6] A. Alcaine, E. Marqués-López, R. P. Herrera, *RSC Adv.* **2014**, *4*, 9856-9865.

[7] There is only one synthetic protocol where the addition of nitroalkanes to *N*-acylhydrazones is carried out under stereoselective control, which requires of stoichiometric amounts of a Lewis acid promoter: J. L. Leighton, R. Berger, S. Shirakawa, G. T. Notte, *US20080167468*, **2008**.

[8] a) F. Fini, V. Sgarzani, D. Pettersen, R. P. Herrera, L. Bernardi, A. Ricci, *Angew. Chem. Int. Ed.* **2005**, *44*, 7975-7978; b) L. Bernardi, F. Fini, R. P. Herrera, A. Ricci, V. Sgarzani, *Tetrahedron* **2006**, *62*, 375-380.

[9] a) K. Kacprzak, J. Gawroński, *Synthesis* **2001**, 961-998; b) S.-K. Tian, Y. Chen, J. Hang, L. Tang, P. McDaid, L. Deng, *Acc. Chem. Res*. **2004**, *37*, 621-631; c) C. E. Song (Ed) *Cinchona Alkaloids in Synthesis and Catalysis*; Wiley-VCH Verlag GmbH & Co. KGaA, **2009**; d) T. Marcelli, H. Hiemstra, *Synthesis* **2010**, 1229-279; e) Q.-F. Wang, *Synlett* **2010**, 163-164; f) E. M. O. Yeboah, S. O. Yeboah, G. S. Singh, *Tetrahedron* **2011**, *67*, 1725-1762; g) L. Jiang, Y.-C. Chen, *Catal. Sci. Technol*. **2011**, *1*, 354–365; h) L. Stegbauer, F. Sladojevich, D. J. Dixon, *Chem. Sci*. **2012**, *3*, 942–958; i) J. Duan, P. Li, *Catal. Sci. Technol*. **2014**, *4*, 311–320; j) L. A. Bryant, R. Fanelli, A. J. A. Cobb, *Beilstein J. Org. Chem.* **2016**, *12*, 429-443; k) S. S. Girija, E. M. O. Yeboah, *Rep. Org. Chem.* **2016**, *6*, 47-75.

[10] To some examples of cinchona-catalyzed aza-Henry reactions, see: a) C. M. Bode, A. Ting, S. E. Schaus, *Tetrahedron* **2006**, *62,* 11499-11505; b) H. Li, X. Zhang, X. Shi, N. Ji, W. He, S. Zhang, B. Zhang, *Adv. Synth. Catal.* **2012**, *354*, 2264-2274; c) A. Parra, R. Alfaro, L. Marzo, A. Moreno-Carrasco, J. L. G. Ruano, J. Alemán, *Chem. Comm.* **2012**, *48*, 9759-9761; d) A. Kumar, J. Kaur, S. S. Chimni, A. K. Jassal, *RSC Adv.* **2014**, *4*, 24816-24819; e) J. Vicario, P. Ortiz, J. M. Ezpeleta, F. J. Palacios, *J. Org. Chem.* **2015**, *80*, 156-164.

[11] C. Cassani, R. Martín-Rapún, E. Arceo, F. Bravo, P. Melchiorre, *Nat. Protoc.* **2013**, *8*, 325-344.

[12] D. Salvador-Gil, L. Ortego, R. P. Herrera, I. Marzo, M. C. Gimeno, *Dalton Trans.* **2017**, *46*, 13745-13755.

[13] CCDC-1961464 for (*S*)-**4ga** and CCDC-1961465 for (*R*)-**4ga** contain the supplementary crystallographic data for this paper. These data can be obtained free of charge from The Cambridge Crystallographic Data Centre via www.ccdc.cam.ac.uk/data_request/cif

[14] a) J. Boruwa, N. Gogoi, P. P. Saikia, N. C. Barua, *Tetrahedron: Asymmetry* **2006**, *17*, 3315-3326; b) C. Palomo, M. Oiarbide, A. Laso, *Eur. J. Org. Chem.* **2007**, 2561-2574; c) Y. Alvarez-Casao, E. Marqués-López, R. P. Herrera, *Symmetry* **2011**, *3*, 220-245.

[15] The concentration of reagent **1h** in the reaction medium was determined by ^{1}H-NMR spectroscopy, employing mesitylene as internal standard (Section 4. Kinetic experiments in supporting information).

[16] J. Casado, M. A. Lopez-Quintela, F. M. Lorenzo-Barral, *J. Chem. Educ.* **1986**, *63*, 450-452.

[17] a) J. E. Dixon, T. C. Bruice, *J. Am. Chem. Soc.* **1970**, *92*, 905-909; b) F. G. Bordwell, W. J. Boyle, *J. Am. Chem. Soc.* **1975**, *97*, 3447-3452; c) J. V. Alegre-Requena, E. Marqués-López, R. P. Herrera, *Chem. Eur. J.* **2017**, *23*, 15336-15347; d) J. V. Alegre-Requena, E. Marqués-López, R. P. Herrera, *ACS Catal.* **2017**, *7*, 6430-6439.

[18] a) L. Simón, R. S. Paton, *J. Org. Chem.* **2015**, *80*, 2756-2766; b) M. N. Grayson, K. N. Houk, *J. Am. Chem. Soc.* **2016**, *138*, 1170-1173.

[19] For other different mechanistic proposals, see: a) Y. Sohtome, N. Takemura, K. Takada, R. Takagi, T. Iguchi, K. Nagasawa, *Chem. Asian J.* **2007**, *2*, 1150-1160; b) X. Chen, J. Wang, Y. Zhu, D. Shang, B. Gao, X. Liu, X. Feng, Z. Su, C. Hu, *Chem. Eur. J.* **2008**, *14*, 10896-10899; c) L. Belding, S. M. Taimoory, T. Dudding, *ACS Catal.* **2015**, *5*, 343-349; d) J. V. Alegre-Requena, E. Marqués-López, R. P. Herrera, *Adv. Synth. Catal.* **2016**, *358*, 1801-1809; e) J. Otevrel, P. Bobal, *J. Org. Chem.* **2017**, *82*, 8342-8358; f) T. Kumpulainen, J. Qian, A. M. Brouwer, *ACS Omega* **2018**, *3*, 1871-1880.

[20] K. Fukui, *Acc. Chem. Res.* **1981**, *14*, 363-368.

[21] E. Kraka, D. Cremer, *Acc. Chem. Res.* **2010**, *43*, 591-601.

[22] a) Gaussian 16, Revision B.01, M. J. Frisch, G. W. Trucks, H. B. Schlegel, G. E. Scuseria, M. A. Robb, J. R. Cheeseman, G. Scalmani, V. Barone, G. A. Petersson, H. Nakatsuji, X. Li, M. Caricato, J. Marenich, A. Bloino, B. G. Janesko, R. Gomperts, B. Mennucci, H. P. Hratchian, J. V. Ortiz, A. F. Izmaylov, J. L. Sonnenberg, D. Williams-Young, F. Ding, F. Lipparini, F. Egidi, J. Goings, B. Peng, A. Petrone, T. Henderson, D. Ranasinghe, V. G. Zakrzewski, J. Gao, N. Rega, G.

Zheng, W. Liang, M. Hada, M. Ehara, K. Toyota, R. Fukuda, J. Hasegawa, M. Ishida, T. Nakajima, Y. Honda, O. Kitao, H. Nakai, T. Vreven, K. Throssell, Jr., J. A. Montgomery, J. E. Peralta, F. Ogliaro, M. Bearpark, J. J. Heyd, E. Brothers, K. N. Kudin, V. N. Staroverov, T. Keith, R. Kobayashi, J. Normand, K. Raghavachari, A. Rendell, J. C. Burant, S. S. Iyengar, J. Tomasi, M. Cossi, J. M. Millam, M. Klene, C. Adamo, R. Cammi, J. W. Ochterski, R. L. Martin, K. Morokuma, O. Farkas, J. B. Foresman, D. J. Fox, Gaussian, Inc., Wallingford CT, **2016**. For references of the ωB97X-D functional: b) A. D. Becke, *J. Chem. Phys*. **1997**, *107*, 8554-8560; c) J.-D. Chai, M. Head-Gordon, *Phys. Chem. Chem. Phys*. **2008**, *10*, 6615-6620. For references of the 6–311G(d) basis set: d) W. J. Hehre, R. Ditchfield, J. A. Pople, *J. Chem. Phys*. **1972**, *56*, 2257-2261; e) P. C. Hariharan, J. A. Pople, *Theoret. Chim. Acta* **1973**, *28*, 213-222; f) R. Krishnan, J. S. Binkley, R. Seeger, J. A. Pople, *J. Chem. Phys*. **1980**, *72*, 650-654; g) A. D. McLean, G. S. Chandler, *J. Chem. Phys*. **1980**, *72*, 5639-5648; h) M. M. Francl, W. J. Pietro, W. J. Hehre, J. S. Binkley, M. S. Gordon, D. J. DeFrees, J. A. Pople, *J. Chem. Phys*. **1982**, *77*, 3654-3665; i) V. A. Rassolov, M. A. Ratner, J. A. Pople, P. C. Redfern, L. A. Curtiss, *J. Comp. Chem*. **2001**, *22*, 976-984. For references of the Def2-QZVPP basis set: j) F. Weigend, R. Ahlrichs, *Phys. Chem. Chem. Phys*. **2005**, *7*, 3297-3305; k) F. Weigend, *Phys. Chem. Chem. Phys*. **2006**, *8*, 1057-1065. For references of the SMD solvation model: l) E. Cancès, B. Mennucci, J. Tomasi, *J. Chem. Phys*. **1997**, *107*, 3032-3041; m) B. Mennucci, E. Cancès, J. Tomasi, *J. Phys. Chem*. B. **1997**, *101*, 10506-10571; n) B. Mennucci, J. Tomasi, *J. Chem. Phys*. **1997**, *106*, 5151-5158; o) J. Tomasi, B. Mennucci, E. Cancès, *J. Mol. Struct. THEOCHEM* **1999**, *464*, 211-226; p) G. Scalmani, M. J. Frisch, *J. Chem. Phys*. **2010**, *132*, 114110-114115; q) A. V. Marenich, C. J. Cramer, D. G. Truhlar, *J. Phys. Chem. B*. **2009**, *113*, 6378-6396.

[23] GoodVibes, version 3.0.0. G. Luchini, J. V. Alegre-Requena, Y. Guan, I. Funes-Ardoiz, R. S. Paton. http://doi.org/10.5281/zenodo.595246, **2019**.

[24] Berkeley Madonna, version 9.1.3. R. Macey, G. Oster, T. Zahnley. University of California Berkeley, **2018**.

[25] a) P. I. Pollak, D. Y. Curtin, *J. Am. Chem. Soc.* **1950**, *72*, 961-965; b) J. I. Seeman, *Chem. Rev*. **1983**, *83*, 83-134.

[26] Q. Peng, F. Duarte, R. S. Paton, *Chem. Soc. Rev.* **2016**, *45*, 6093-6107.

[27] Hydrazone **1o** has been chosen because we do not know its experimental outcome (to be compared with the computational predictions) and because it has a *t*Bu substituent, which contains three Me groups and leads to a smaller conformational space compared to other substituents such as *i*Pr or Et.

[28] a) S. T. Schneebeli, M. L. Hall, R. Breslow, R. Friesner, *J. Am. Chem. Soc.* **2009**, *131*, 3965-3973; b) It is worth to mention that the authors used zero-point (ZP)-corrected electronic energy (E) values instead of G. For this reason, we calculated $\Delta\Delta G^{\ddagger}$ using both ZP-corrected E and G in case the calculated values dramatically changed from one protocol to the other, but the differences observed were lower than 0.5 kcal·mol^{-1} when comparing both approaches (Table S7). The DFT errors of selectivity calculations might appear from multiple sources, including lack of explicit solvent molecules in the simulations, basis set superposition and incompleteness errors (BSSE and BSIE) and accuracy of the implicit solvation models, among others, and they are very challenging, if not impossible, to correct when working with relatively complex systems.

[29] a) H. Miyabe, Y. Takemoto, *Bull. Chem. Soc. Jpn.* **2008**, *81*, 785-795; b) S. J. Connon, *Chem. Commun.* **2008**, 2499-2510; c) I. G. Sonsona, E. Marqués-López, R. P. Herrera, *Beilstein J. Org. Chem.* **2016**, *12*, 505-523.

[30] R. P. Herrera, D. Roca-López, G. Navarro-Moros, *Eur. J. Org. Chem.* **2010**, 1450-1454.

[31] E. Marqués-López, E. Díez, E. Martín-Zamora, E. Álvarez, R. Fernández, J. M. Lassaletta, *Synlett* **2012**, *23*, 885-888.

[32] C. G. Oliva, A. M. S. Silva, D. I. S. P. Resende, F. A. A. Paz, J. A. S. Cavaleiro, *Eur. J. Org. Chem.* **2010**, 3449-3458.

[33] a) J. V. Alegre-Requena, E. Marqués-López, R. P. Herrera, *RSC Adv.* **2015**, *5*, 33450-33462; b) J. V. Alegre-Requena, E. Marqués-López, R. P. Herrera, *WO2016005407,* **2016**.

[34] W. Yang, D.-M. Du, *Org. Lett.* **2010**, *12*, 5450-5453.

10.1002/chem.202000232

Entry for the Table of Contents (Please choose one layout)

Layout 2:

FULL PAPER

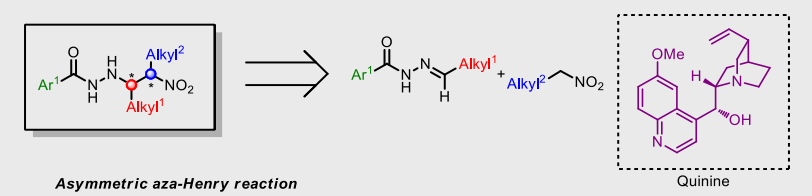

The first asymmetric catalyzed aza-Henry reaction of hydrazones is presented. In this process, quinine was used as catalyst to synthesize a variety of alkyl substituted β-nitrohydrazides with up to 94% ee. Additionally, experimental and *ab initio* studies were performed to understand the reaction mechanism. The results revealed a concerted mode of activation in which a C-C bond forming reaction and a protonation occur simultaneously.

Isaac G. Sonsona,[a] Juan V. Alegre-Requena,[a] Eugenia Marqués-López,[a] M. Concepción Gimeno[b] and Raquel P. Herrera*[a]*

Page No. – Page No.

Asymmetric organocatalyzed aza-Henry reaction of hydrazones: experimental and computational studies